Research Square

Preprints are preliminary reports that have not undergone peer review.
They should not be considered conclusive, used to inform clinical practice,
or referenced by the media as validated information.

Time as a design variable: a computable criterion for matching release to a staged pathology, demonstrated in spinal cord injury

Jiongli Kuang

College of Medicine, Southwest Jiaotong University https://orcid.org/0009-0005-3015-7660

Wenchun Wang

wwc1977biology@163.com

Department of Rehabilitation Medicine, The General Hospital of Western Theater Command https://orcid.org/0000-0001-9742-9089

Research Article

Keywords: controlled release, release kinetics, stimuli-responsive hydrogel, time-programmable, sequential release, spinal cord injury

Posted Date: November 3rd, 2026

DOI: https://doi.org/10.21203/rs.3.rs-11597192/v1

License: This work is licensed under a Creative Commons Attribution 4.0 International License. Read Full License

Additional Declarations: The authors declare no competing interests.

Abstract

Controlled release is usually specified by rate and duration, not by whether it is timed to the pathology it interrupts. Spinal cord injury (SCI) is a case in point: a staged cascade on which most therapies act only once. We advance a “time-programmable” design philosophy—hydrogels matched in timing and sequence to the pathology—defined by three criteria: (a) pre-encoded, temporally ordered response events; (b) logical gating of later events by earlier ones; (c) verifiable alignment of event timing with that timeline. Using the pathology as the coordinate, we dissect hydrogel design principles—contrasting single-response with multi-stage cascade logic and identifying threshold, kinetics and degradation window as the parameters of matching. We then examine how hydrogels intervene across four mechanisms: inflammation, oxidative stress, glial scarring and axonal regeneration. The chronic stage is targeted by six of the fifty-seven systems, yet one program is designed to terminate there, and it misses that window by eleven days. Twenty-three are built for the acute window: its excitotoxic phase is over before surgery (median decompression 28–67 h), though its oxidative phase persists for days. Across the 57 systems the pattern inverts clinical need: release is built for the phase least reachable in practice, not for the chronic window that can be entered electively. Eleven of the thirteen Level II systems order events by the material's own clock, not a pathological cue. A temporal matching index, applied to the seven systems with release data, places two above 0.6 — a gap between ambition and execution.

1. Introduction

Controlled release has long been organized by its kinetics: sustained, zero-order, pulsatile or triggered, and by the duration over which a dose is delivered. What this vocabulary does not capture is whether release is timed to the biology it is meant to interrupt. When the target is a single process, the omission is harmless; when the target is a cascade, it is decisive.

Spinal cord injury (SCI) remains among the most devastating conditions in neurology, producing irreversible motor, sensory, and autonomic dysfunction and a lifelong burden on patients and society [1]. As survival has improved, the prevalent population living with chronic disability continues to expand [2, 3]. Current management—early decompression, hemodynamic support, rehabilitation—mitigates secondary complications but does not restore lost connectivity [4]. This durable failure reflects a fundamental property of SCI: it is not a single event but a dynamic, temporally orchestrated cascade whose therapeutic requirements change as it unfolds [5].

The pathophysiology of SCI is conventionally divided into primary and secondary phases. The primary injury is the immediate mechanical insult—compression, contusion, or laceration—that severs axons, ruptures vasculature, and triggers hemorrhage and ischemia [6, 7]. This initiates the secondary injury cascade, the principal target of therapeutic intervention, which is itself staged [8]: an acute window (1–72 h) dominated by reactive oxygen species (ROS), excitotoxicity, and oxidative cell death [9, 10]; a subacute phase (days to weeks) of inflammatory infiltration and astrogliosis [11, 12]; and a chronic phase (weeks to months) in which a glial scar and cystic cavities consolidate as barriers to regeneration [13, 14]. Critically, these events are sequential, and each stage is governed by a distinct molecular microenvironment.

This temporal heterogeneity defines the central therapeutic challenge: a single-point intervention—a bolus of a neuroprotective drug, a single growth factor, or a passive scaffold—is inherently mismatched to a pathology that changes over time [15]. An agent that scavenges ROS acutely may be inert or detrimental once glial scarring becomes the dominant obstacle; a regenerative factor delivered prematurely may be cleared before its window arrives [16, 17]. This has motivated a paradigm shift from “what to deliver” toward “when, and in what sequence, to deliver” [18]—an imperative already codified clinically as “time is spine” [19]. An effective therapy must therefore be spatiotemporally matched, its action aligned in both location and time with the evolving microenvironment [20].

Hydrogels have emerged as the leading biomaterial platform for SCI repair owing to their high water content, tissue-like mechanics, injectability, and capacity to encapsulate and release therapeutic cargo [3, 6]. Within this field, stimuli-responsive hydrogels—releasing payloads in response to endogenous cues (ROS, pH, enzymes) or exogenous stimuli (light,

temperature, magnetic fields)—promise on-demand, microenvironment-dependent delivery [5, 7]. Yet a critical gap persists: the majority are single-response systems that engage at one point in the timeline [8, 9], and the reviews surveying this field have catalogued materials by response type rather than by their alignment with the temporal logic of SCI [5, 6]. The field therefore lacks a coherent framework for evaluating whether material response is matched to pathology in time.

This review advances the central thesis that the therapeutic value of responsive hydrogels for SCI lies not in whether they respond, but in when and in what sequence they respond—that is, in their ability to match material response to the spatiotemporal pathology of the injured cord. We term such systems **time-programmable hydrogels**. To move this term from a rhetorical slogan to an operational criterion, we define it by three jointly necessary, individually verifiable conditions:

1. **(a) Encoding existence.** The material must actively pre-encode at least two response events arranged in a deliberate temporal order. A single stimulus-triggered release—however microenvironment-sensitive—does not qualify, because it embodies no temporal *program*, only a temporal *point*.
2. **(b) Order constraint.** The later event must be *ordered after*, rather than merely coexist with, the earlier one. Two mechanisms satisfy this requirement, and they define two distinct programming routes. The first is *hard gating*: a later event is chemically triggered only once (or after) the earlier event has occurred—for example, MMP-gated release of a growth factor that becomes accessible only after ROS-triggered disruption of the network. The second is *engineered sequencing*: the later event is assigned a release kinetics deliberately slower than the earlier one, so that its action is scheduled to begin only as the earlier event recedes. What is excluded by (b) is not the *mechanism* of ordering, but the *absence* of ordering—systems in which two payloads merely coexist with independent, parallel release curves and no deliberate temporal relationship between them. Juxtaposition is not sequence.
3. **(c) Temporal matching.** The time coordinates of the encoded events must be *explicitly* aligned with the pathological timeline (Section 3) and amenable to quantitative verification—for instance, by demonstrating that each payload is released at concentrations and times that coincide with its designated pathological window.

Under these criteria, a given hydrogel can be classified as time-programmable or not by inspection. Two systems already exemplify these two routes — a chemically gated ROS→MMP cascade [21] and a kinetically scheduled dual-phase scaffold [22] — and their emergence signals the field's transition from single-point responsiveness toward multi-stage temporal coordination.

It is essential to distinguish time-programmable from the closely related self-adaptive design. A recent framework defines self-adaptive hydrogels as materials that “recognize the dynamic pathological cues within the lesion microenvironment, and undergo programmable adjustments to their structural and functional properties” [23]. That framework is a substantial advance, and it organizes the literature in a coherent way: materials are grouped by the pathological stage they are built to address, which makes the field's coverage of each stage immediately legible, and it is the reference against which any new classification has to be judged.

Its analytical unit, however, is the stage, and a stage-based classification cannot answer a different question: whether the second of two events is actually constrained by the first. Two systems filed under the same stage may differ in precisely this respect. A two-step ROS→MMP cascade [21] and a dual-phase polymer carrying two payloads [22] both address the transition from inflammation to regeneration, and a stage-based framework would place them together. In the first, the second release is unlocked by a chemical change produced by the first; in the second, it is merely scheduled later. Our conditions keep both in view but separate them: [21] satisfies (a) and (b) fully and (c) only in part, whereas [22] satisfies (a) but only weakly (b), because its second release is determined by kinetics rather than by the first event.

The decisive contrast—between *scheduled* and *gated* sequences—is the classification on which our entire analysis of therapeutic timing rests, and it is illustrated by a self-adaptive nanomedicine (RHNP), which, although not a hydrogel, follows the same self-adaptive logic and switches its targeting moiety through ROS-sensitive bonds but encodes no multi-step order, remaining one step below the time-programmable threshold [24].

In this review, we develop the time-programmable framework in full. We first articulate the spatiotemporal pathophysiology of SCI as the coordinate system for material design (Section 3); analyze the design principles of stimuli-responsive hydrogels, contrasting single-response and cascade logic and identifying threshold, kinetics, and degradation window as the governing parameters (Section 4); examine how temporally orchestrated hydrogels intervene across the four core mechanisms of inflammation, oxidative stress, glial scarring, and axonal regeneration (Section 5); and survey representative systems across response modalities (Section 6). We conclude that the field's next frontier is multi-step cascades spanning three or more distinct pathological stages—bridging the structurally unclaimed chronic-phase glial-scarring endpoint to complete the temporal chain from acute neuroprotection to regenerative support (Section 7).

The claim this review defends. Stripped of detail, the argument is a single empirical statement that can be checked against Supplementary Table S1. Twenty-three of the fifty-seven coded systems are built to act in the acute window, whose excitotoxic phase is over before a patient reaches the operating theatre; six are built for the chronic window, the only stage that can be entered electively; and of those six, one is designed to end there, releasing its scar-directed payload at a half-time of 3.1 days, eleven days before the window it targets opens. The field's temporal effort is therefore concentrated where clinical timing makes it hardest to apply and thin where it is easiest. The review then asks whether that pattern is a property of the materials or of the question they were asked to answer, and supplies three criteria and an index that make the answer checkable rather than rhetorical.

2. Literature search strategy and bibliometric methods

This review is a **focused critical review** of time-programmable hydrogels for SCI. Rather than attempting an exhaustive enumeration of the field, we deliberately adopt a purposive sampling strategy: a core set of 57 representative systems—assembled by directed searching, reference-list snowballing, and a structured PRISMA-style database search—is used to anchor a critical analysis of design principles and to exemplify each response modality, and this set does not claim to capture every responsive hydrogel reported for SCI. The structured database search is reported transparently to make the evidence base reproducible; the search was supplemented by post-search tracking of late-2025/2026 literature so that the most recent sequentially releasing and chronic-stage systems are not omitted. We make no claim of systematic-review completeness, and we do not compute coverage proportions that would imply representativeness; the Fig. 1 heatmap is instead a descriptive snapshot of the curated set that renders the chronic-stage gap and the single-response-to-cascade transition visible.

2.1 Search strategy

We searched PubMed/MEDLINE, Web of Science (Core Collection) and Scopus on 22–23 October 2026 for records published between 1 January 2015 and the search date. The lower bound reflects when stimuli-responsive, sequentially releasing hydrogel design crystallised as a distinct paradigm; the upper bound was extended to 2026 to capture the most recent systems. The search combined three concept blocks — disease, material class, and responsiveness or sequential release — joined by Boolean AND, and the database-specific strings are given in the Supplementary search log; reference lists of included studies and recent reviews were also hand-searched.

The resulting evidence base is a purposive sample of 57 original research articles reporting *in vivo* data, assembled from directed searching, snowballing and late-2025/2026 tracking. Snowballing excluded one non-hydrogel nanocarrier [26] and one predominantly *in vitro* study [27], and the seven most recent additions include the injectable hyaluronan carrier of [28]. It is listed study by study in Supplementary Table S1, and that list is the operational definition of N used throughout this review. Table 1 breaks the citation base down by role: the 57 included studies, 8 orientation reviews, and the background, coverage and mechanistic references that support the argument in Sections 3 to 7.

2.2 Inclusion and exclusion criteria

Inclusion criteria: (i) original research articles reporting the design, characterization, and therapeutic evaluation of a hydrogel for spinal cord injury in which at least one payload is released over a defined time course; (ii) that time course is ordered by at least one of: (a) a stimulus-responsive element; (b) a temporally staged or sequentially released payload; or (c) a defined affinity- or charge-mediated retention mechanism; and (iii) the study reports *in vivo* outcomes (functional, histological, or molecular) in SCI models, so that *in vitro*-only studies are excluded from N but may be cited as supporting mechanistic evidence where explicitly linked to an included *in vivo* system. By these criteria the included set is restricted to primary research reporting original *in vivo* data: review articles, which summarize rather than generate *in vivo* results, do not satisfy criterion (iii) and are therefore **excluded from N**; the eight background reviews and methodological syntheses used to position this work within the field ([3, 5–7, 13, 23, 29, 30]) are cited as background and orientation literature only, not as included studies. Criterion (ii) is deliberately broader than stimulus-responsiveness alone. Because the analytical unit of this review is the ordering relation between events rather than the trigger itself (Section 4.2), systems whose ordering is passive, affinity-based or kinetically programmed are admitted—and are identified as such in Supplementary Table S1—rather than excluded; a review that admitted only stimulus-responsive systems could not compare gated with open-loop designs, and that comparison is the argument the review is built on.

Exclusion criteria

(i) hydrogels without any responsiveness or temporal-release feature (passive scaffolds); (ii) non-hydrogel biomaterials (films, conduits, nanoparticles without a hydrogel matrix); (iii) studies of hydrogels for other CNS or peripheral indications without SCI data; (iv) conference abstracts, editorials, and non-peer-reviewed sources; and (v) duplicate records across databases.

2.3 Selection flow

Records were screened in a PRISMA-style flow, reported as a reproducible record rather than as a claim of systematic-review completeness. The three database queries returned 465 records (PubMed 70, Web of Science 238, Scopus 157); 280 remained after de-duplication by DOI; 51 were excluded at title and abstract, leaving 229 assessed in full text; 174 were excluded at that stage, leaving 55 that met the inclusion criteria; and adding three studies published after the cut-off while removing one duplicate gave the final set of 57. The complete strings, with the date window used for each database, are given in the Supplementary search log. The complete flow, with every intermediate count, is given in Supplementary Fig. S1 and in the Supplementary search log. Coding depth is recorded study by study in Supplementary Table S1: 32 of the 57 entries were coded from the full text, and 25 from the abstract and reference list where the full text was not accessible in a readable form; for the latter, trigger, level and stage were assigned from the design as reported in the abstract, and no entry was coded from its title alone. The proportions reported in Section 2.4 and summarised in the abstract describe this corpus at that depth of coding. The distribution of depth is also informative: every one of the 25 abstract-only entries falls in Level I, and all of them sit in the acute, subacute or regenerative window. The chronic counts and the thirteen Level II systems, which carry the two central claims of the review, are therefore coded entirely from full texts.

Table 1
Composition of the 161-entry reference list.

Category	n	Where the entries are used
Included studies (N)	57	listed study by study in Supplementary Table S1
Orientation reviews	8	Introduction and Section 6
Background mechanism citations	25	Section 3
Coverage citations	20	Sections 2 and 6
Mechanistic and translational citations	51	Sections 4, <link rid="Sec17">5</link> and 7
Total	161	

A broader search, widening only the responsiveness block with the bare terms ROS, reactive oxygen species, antioxidant, nanozyme, conductive, photothermal and near-infrared under the same three-block AND structure, returned 1,044 records (565 unique). It confirms that the field is far larger than the 57 studies selected here, which is why this is a focused critical review and not a systematic one, and why no claim of exhaustive coverage is made.

2.4 Bibliometric scheme: a “response type × pathological stage” heatmap

To move the claim that the chronic stage is structurally unaddressed—rather than merely under-counted—from qualitative impression to an inspectable, citable conclusion, we constructed a two-dimensional distribution matrix (heatmap). Columns encode the four pathological stages defined in Section 3 (acute / subacute / chronic / regenerative), rows encode the seven response chemistries represented in the sample (ROS / pH / enzyme / temperature / magnetic–visible / photo–NIR / none, the last denoting systems ordered passively, by affinity or by kinetics), and the matrix is divided into panels by temporal architecture (Level I, single event; Level II, two or more events in a deliberate order; Level III, a gated chain crossing three or more distinct stages). Each included study is assigned to one trigger chemistry, one architecture and one primary therapeutic target, so it enters the count exactly once; cell entries are raw study counts, with row and column marginals reported to expose distributional structure.

This matrix is descriptive rather than quantitative: because the 57 studies are a purposive sample rather than an exhaustive enumeration, we deliberately do not compute coverage proportions that would imply representativeness. Instead, the heatmap is presented as Fig. 1 (and, with the completed counts, as **Supplementary Table S1**) to expose the distributional structure of the curated set. Two features carry the argument. First, **no staged program delivers its terminal event inside the chronic glial-scarring window**: although ten systems engage that stage and six take it as their primary target, the single two-event program designed to terminate there releases its scar-directed payload long before that window opens (Table 2); the chronic cell is therefore not under-counted but structurally unclaimed. Second, **cascade/sequential systems remain a minority** relative to single-response systems — a pattern that motivates the chronic-stage gap and the multi-step cascade frontier developed in Sections 5.3 and 7.

A note on the column that records this. Supplementary Table S1 lists an *ordering trigger* for every study: the cue, if any, that orders the later event relative to the first. A system whose events are all released by one shared cue is recorded as having none, because that cue cannot order them; response chemistry and ordering chemistry are therefore counted separately, and [32] exemplifies the distinction, being a thrice-released system with a single ROS trigger. The arithmetic behind these claims is worth stating directly. Systems whose ordering is not chemically triggered (n = 18) and ROS-triggered systems (n = 17) together account for 35 of the 57 studies. Only two of the thirteen Level II systems ([21] and [31]) couple their second event to an endogenous cue; the remaining eleven are ordered by release kinetics, electrostatic retention or affinity. All thirteen are Level II in Supplementary Table S1, twelve of them two-event and one three-step ([32], whose third step is surface-presented rather than released).

Three counts are used here with distinct meanings, and 'terminal' refers to the stage a system is designed to end in, not to where its half-release time happens to fall (the latter is measured separately by the TMI): a stage is **engaged** if any element of a system addresses it, is a system's **primary target** if that stage supplies the design's organising rationale, and is **terminal** only for a two-event system whose second event is scheduled within it. On these definitions the chronic stage, although engaged by ten studies, is the primary target of six, and it is the only stage at which a single two-event program is designed to end ([15], whose ordering is kinetic rather than gated)—and even that program does not arrive in time: its scar-directed payload is fully released by day 3, while the chronic window opens at day 14 (Table 2).

3. The spatiotemporal pathophysiology of spinal cord injury: a temporal coordinate system

Any rational design of a time-programmable hydrogel must begin from a precise account of what changes, and when, in the injured spinal cord. This section therefore articulates the staged pathophysiology of SCI not as a static catalogue of molecular events, but as a temporal coordinate system against which material response must be aligned [33, 34]. At each stage we emphasize the biochemical and biophysical signals of the microenvironment—for these are precisely what a responsive hydrogel can be programmed to sense (Fig. 2).

3.1 Primary injury and the acute phase (1–72 h): oxidative stress and excitotoxicity

The primary injury is the immediate mechanical destruction of spinal cord tissue by compression, contusion, laceration or distraction [2, 6]. Within minutes to hours, disrupted vasculature produces haemorrhage, ischemia and oedema, the blood–spinal cord barrier fails, and necrotic cells release their contents into the interstitium [6, 35–37]. This initiates the acute phase of secondary injury, which is dominated by two intertwined and mutually amplifying processes.

Oxidative stress arises from a burst of reactive oxygen species (ROS)—superoxide, hydrogen peroxide, hydroxyl radical and peroxynitrite—produced by mitochondrial dysfunction and by the respiratory burst of infiltrating neutrophils and activated microglia [8, 9]; excess ROS overwhelms endogenous antioxidant defences and drives apoptotic and necrotic death [8, 10]. Excitotoxicity runs in parallel: excessive glutamate release and impaired reuptake activate NMDA and AMPA receptors, and the resulting calcium influx converges on the mitochondrion, where opening of the permeability transition pore turns the organelle into a generator of further ROS [38–40]. The loop is self-amplifying, and it extends to oligodendrocytes and myelinated white matter, contributing to delayed axonal degeneration [38, 41].

For material design, what matters is that this phase offers the richest set of endogenous triggers in the whole timeline—elevated ROS, acidosis from lactic acid accumulation, and early proteolytic activity—each sharply restricted in time. The therapeutic imperative is correspondingly narrow: scavenge ROS, restore ionic homeostasis, and limit the spread of death before the loss becomes irreversible.

3.2 Subacute phase (days to weeks): inflammation and the immune microenvironment

As the acute storm subsides, a massive inflammatory response defines the subacute phase [11, 42]. Neutrophils arrive first, followed by monocyte-derived macrophages and activated resident microglia, which adopt a spectrum of reactive states from homeostatic to neurotoxic [43]; together they release TNF-α, IL-1β and IL-6, while DAMPs from dying cells perpetuate the loop [12, 42]. The response is orchestrated by bidirectional signalling among microglia, astrocytes and infiltrating leukocytes [44], and extends to adaptive immunity, where T and B cells can be pathogenic or reparative depending on antigen specificity [45]. Early inflammation clears debris, but its persistence converts repair into destruction [12].

A central axis is the polarization of macrophages and microglia between M1 and M2 phenotypes [42, 46]: after SCI the M1 state predominates and is actively sustained by the microenvironment, unlike cutaneous healing, where an M1-to-M2 shift occurs [46, 47]. Skewing the balance toward M2 is therefore a major target, and several hydrogels act there—by scavenging DAMPs or by sustained release of IL-10 [11, 48, 49]. The dichotomy is nonetheless an *in vitro* construct: single-cell sequencing shows microglia undergoing permanent reprogramming into a disease-associated state that supports recovery, and macrophages resolving into subpopulations that map onto neither pole [47, 50, 51] (Section 5.1). The signals available for sensing at this stage are declining ROS, elevated cytokines, and rising MMPs as the lesion moves toward chronicity [13].

3.3 Chronic phase (weeks to months): glial scar formation and cystic cavitation

The chronic phase consolidates two barriers: the glial scar and the cystic cavity [14, 52]. Reactive astrogliosis, driven in part by M1-polarized microglia, builds a dense network of hypertrophic astrocytes interwoven with fibroblasts, pericytes and deposited matrix [48, 52]; reactivity is itself heterogeneous, and activated microglia can induce a neurotoxic astrocyte state that kills neurons and oligodendrocytes [53, 54]. The scar blocks growth cones and secretes CSPGs that repel them [48, 55]. CSPGs accumulate in the lesion and persist for months, and degrading their glycosaminoglycan chains with chondroitinase ABC promotes recovery, establishing them as the tractable inhibitory cue [55–57]. The inhibition is receptor-mediated—PTPσ binds CSPGs and transduces the repulsive signal, and its deletion lets axons enter CSPG-rich regions [58]—while tissue loss and inadequate matrix support produce cystic cavitation [52].

The scar is not purely detrimental: genetic ablation shows that reactive astrocytes also confine cytotoxic inflammation and preserve spared tissue [59], and scar formation can, under some conditions, aid axon regeneration [60]. The goal is therefore not ablation but temporal and spatial modulation. Yet responsive hydrogels remain thinnest precisely here—a gap returned to in Sections 5.3 and 6—and the targets of emerging interest are the integrin–N-cadherin pathway driving astrocyte aggregation [14] and Pin1, which promotes astrocyte proliferation through PI3K/AKT/CDK2 [16].

3.4 The regenerative phase: neural stem cell mobilization, axonal regeneration, and remyelination

Superimposed on, and partly opposed by, these inhibitory processes is a regenerative phase in which endogenous repair must be mobilized [22]. NSPCs can in principle give rise to neurons and oligodendrocytes, but in the injured cord they preferentially adopt astrocytic fates [60, 61]; axonal regeneration is further limited by the absence of growth-promoting substrates, by inhibitory cues, and by the intrinsic inability of many CNS neurons to sustain growth programs [22], while remyelination by OPCs is inefficient in the chronic lesion [61].

The imperative is therefore threefold: bias NSPC fate toward neurons, provide neurotrophic support for extension and myelination, and restore vascular supply [61, 62]. Anderson and colleagues showed that only the combination of three interventions—neuronal reprogramming, a growth-factor-releasing hydrogel, and a chemoattractant gradient—drove robust regrowth across a complete lesion [62]. Because such signals act only once the acute storm has subsided, delivery must be sequential rather than simultaneous—the requirement the strategies of Section 4 are built to satisfy.

3.5 The temporal logic distilled: why “when” matters

Four stages, four imperatives: scavenge early, resolve inflammation next, modulate the scar in the middle, and support regeneration last. Because the molecules that define each stage—ROS, cytokines, MMPs, CSPGs—are also the ones that appear and recede most sharply, they are at once the pathology and the only clock a material can read (Fig. 2). To make that clock usable, we fix the four windows numerically and use them unchanged for every count and every score that follows: acute 1–72 h, subacute 72 h–14 days, chronic 14 days–12 weeks, regenerative from roughly two weeks onward, overlapping the chronic window rather than succeeding it—the chronic window being the interval over which the scar matures and consolidates (Section 3.3). The lower bound of the acute window is taken as 1 h rather than zero so that W is a finite ratio; the injury instant itself is not a sampling interval, and this choice affects only the one payload scored against this

window. Because the regenerative stage shares the chronic interval rather than following it, payloads whose target is regenerative are scored against the chronic window, which is why the nomogram has three panels and not four. That is the foundation on which the remainder of this review builds.

The four stages are not sequential compartments. They overlap: the regenerative axis opens while the chronic barrier is still consolidating, and inflammation persists into the subacute period rather than resolving at a boundary. **This overlap, not any single transition, is what a staged material has to negotiate** - and it is why the framework developed below is built on windows rather than on stages.

4. Design principles of time-programmable hydrogels

Section 3 established the temporal coordinate system of SCI pathology; we now ask how a hydrogel can be engineered to sense and respond to that pathology in the correct temporal order. This section develops the answer in three steps: a taxonomy of the available response modalities; the crucial distinction between single-response systems and multi-stage cascade logic; and the key design parameters—response threshold, release kinetics, and degradation window—that determine whether a given design achieves true temporal matching.

Before the modalities are examined, one quantity should be named, because everything that follows is a statement about it. Classical release models describe how much is released at time *t*: zero-order gives a constant rate, first-order an exponential approach with a characteristic time, and Higuchi a square-root dependence on *t*. None of them says whether that release is well timed. We therefore work with a dimensionless ratio, $\tau = t_{½}/W$, in which $t_{½}$ is the measured half-release time and W the width of the window the payload is meant to serve: $\tau < 1$ means the payload is spent before its window opens, $\tau \approx 1$ that it spans the window. The remainder of this section uses τ to separate chemically gated from kinetically scheduled designs (4.2) and to derive a matching index that can be computed from a published curve (4.3). The material foundations of this analysis are well established — from growth-factor delivery platforms and microenvironment-responsive design [63–65], through conductive and macromolecule-based release [66, 67] and the design criteria that define smart nerve-repair hydrogels [68], to drug-loaded and peptide- or protein-based strategies [69–71] with emerging cell-functionalization [72], the field surveys of [73, 74], architecturally engineered sequential-release systems [75], and the reviews that map scaffold parameters onto regeneration [76–78]. Our purpose here is not to re-derive them but to organise them around the temporal axis they rarely make explicit.

4.1 Response modalities: a taxonomy of endogenous and exogenous triggers

Stimuli-responsive hydrogels for SCI can be organized along two axes: the source of the trigger (endogenous versus exogenous) and the nature of the response (chemical degradation, physical transition, or electrical/mechanical actuation) [5, 18]. Endogenous triggers are biochemical or biophysical signals that arise naturally in the injured cord and are therefore inherently staged with the pathology; exogenous triggers are applied from outside and offer precise temporal control but require external instrumentation.

Endogenous triggers. The acute-phase oxidative microenvironment provides the most widely exploited endogenous signal in the studies surveyed here: elevated ROS. ROS-responsive hydrogels typically incorporate ROS-cleavable linkers (e.g., thioketal, arylboronic ester, or phenylboronic acid ester bonds) or ROS-scavenging nanomaterial payloads (e.g., MnO_2, nanoselenium, or ZnO-based nanozymes) that either degrade to release cargo or directly neutralize ROS [8, 9]. A representative system is the phenylboronic-acid-modified hyaluronic acid hydrogel that immobilizes engineered extracellular vesicles and releases them on demand in response to ROS [10]. Acidic pH, arising from ischemia-induced lactic acidosis, is a second acute-phase cue; ZIF-8 (a zinc-based metal-organic framework) is the workhorse here, dissociating in acidic microenvironments to release Zn^{2+} and any co-loaded drug [9, 29]. Enzyme-responsive systems exploit the upregulation of matrix metalloproteinases (MMPs), particularly MMP-2/9, which accumulate as the lesion transitions toward chronicity;

MMP-cleavable peptide sequences (e.g., PLGLAG) enable enzyme-triggered release of growth factors such as VEGF or bFGF [13, 30]. More recently, hyaluronidase—persistently elevated in the injured cord—has been exploited as an alternative enzyme trigger [18]. These endogenous cues are attractive precisely because they are temporally aligned with specific pathological stages: ROS and low pH peak acutely, whereas MMPs rise subacutely-to-chronically (Section 3).

Exogenous triggers. Exogenous stimuli—light (near-infrared, NIR), temperature, and magnetic/electric fields—offer on-demand, clinician-controlled temporal control that is independent of the often-heterogeneous endogenous microenvironment [7, 18]. NIR-responsive systems combine photothermal conversion with payload release, as exemplified by ZnO-ZIF8 nanozyme hydrogels in which NIR irradiation accelerates ROS scavenging and Zn^{2+} release [9]. Thermoresponsive hydrogels, such as chitosan/β-glycerophosphate systems that gel at physiological temperature, provide a minimally invasive delivery depot and sustained release [6, 16]. Magnetic- and electric-field-responsive hydrogels—including aligned magnetic nanofiber hydrogels and magneto-electric Fe_3O_4@$BaTiO_3$ composites—generate remote, non-invasive electrical stimulation that promotes neuronal differentiation and M2 macrophage polarization [17, 20]. The trade-off is clear: exogenous triggers offer precise timing but require external apparatus and may face translation barriers, whereas endogenous triggers are self-timed but depend on the fidelity of the pathological signal.

4.2 The core logic: single-response versus cascade (sequential) release

The central design question for a time-programmable hydrogel is not which trigger to use, but how many triggers, and in what order. We distinguish three levels of temporal sophistication (Fig. 3):

1. **(i) Single-response systems.** These systems sense one cue and release one payload at one point in the timeline. They dominate the current literature and are appropriate when the therapeutic goal is confined to a single stage—for example, ROS-triggered neuroprotection in the acute phase [8, 10], or MMP-triggered growth-factor delivery in the subacute-to-chronic transition [13, 30]. Their limitation is structural: because they act only once, they cannot match a pathology that changes character over time.
2. **(ii) Dual-phase and cascade systems.** These systems program two (or more) temporally distinct responses, and they represent the current frontier. Two distinct strategies are emerging, and their distinction is important. The first is a **chemical cascade**, in which one endogenous trigger hands off to another as the microenvironment evolves: the archetype is the ROS→MMP hydrogel (PVA/TSPBA delivering CNT@MnO_2/VEGF), which first releases ROS-scavenging nanodrugs on ROS exposure and later releases VEGF on MMP accumulation, thereby matching the acute oxidative phase and the later regenerative phase within a single injection [21]. The second is a **release-kinetics strategy**, in which temporal programming is achieved not by sequential triggers but by differential release rates from a single scaffold: the dual-phase SilMA hydrogel releases angiotensin-(1–7) rapidly for early M2 polarization while neurotrophin-3 is released slowly from PLGA microspheres for later neuronal differentiation [22]. These two strategies are complementary rather than competing—the former leverages the pathology's own temporal logic, while the latter offers a simpler, more robust route to staged delivery that does not depend on the fidelity of endogenous signals.
3. **(iii) Multi-step (> 2) cascades.** Beyond two stages lies the conceptual end-point of the field: a hydrogel that sequentially addresses three or more *distinct pathological stages or mechanisms* (e.g., ROS → inflammation → glial scar → regeneration) in the correct order. Here the word “multi-step” denotes the number of *mechanistic stages spanned*, not merely the number of temporally ordered release events: a system that stages three events—even three correctly ordered events—within a single mechanistic axis (for example, three successive steps of immune modulation) remains a Level II cascade in our taxonomy, whereas Level III requires that the temporal chain *crosses* at least three different pathological stages or mechanisms. We identified no such system — one that spans three or more distinct stages — among the 57 included studies, and this absence—together with the thin coverage of the chronic glial-scarring stage noted in Section 3.3—defines the clearest opportunity and the most forward-looking challenge for the field (Section 7).

This hierarchy reframes the entire review: among the 57 studies surveyed here, most responsive-hydrogel reports for SCI belong to level (i), a small but growing number exemplify level (ii), and level (iii) remains aspirational. The progression from (i) to (iii) is, in our view, the central trajectory of the field.

Boolean logic gating as the enabling chemistry. A crucial principle underpinning the single-response → cascade transition—and, in particular, condition (b) of our definition—is the engineering of hydrogels that respond only to *specific combinations* of cues. This has been most rigorously developed in the broader responsive-materials literature, where "logic-gated" hydrogels encode Boolean operators directly into their crosslink chemistry [79]: Badeau and colleagues built a modular framework in which stimuli-labile moieties were arranged so that payload release occurred only when a specified logic statement was satisfied, enabling sequential, environmentally stimulated release [79], later extended to logic-based release of site-specifically modified proteins and live-cell cargo [80]. Such Boolean gating is precisely the chemical realization of condition (b): it converts a material that passively degrades into one that *computes* whether the ordered conditions have been met. Complementing this, supramolecular and dynamic-covalent crosslinks—reversible bonds with tunable exchange kinetics—provide the material foundation for programmable responses [81, 82], and general design frameworks offer systematic guidance for selecting inputs, response profiles, and logic schemes [83]. These advances, though largely demonstrated outside SCI, define the chemical repertoire from which time-programmable SCI hydrogels will be assembled—an open opportunity this review highlights.

4.3 Key design parameters: threshold, kinetics, and degradation window

Whether a given responsive design achieves genuine temporal matching depends on three engineering parameters, each of which must be aligned with the pathological timeline established in Section 3 [3, 18]. Figure 4 summarizes how these parameters, together with the choice of responsive elements, translate a single-injection hydrogel into staged, pathology-timed delivery. These parameters correspond to the tunable degrees of freedom identified in systematic design frameworks for stimuli-responsive hydrogels—material composition, crosslinking chemistry, and degradation mechanism—which jointly determine the network's release profile [84].

Response threshold. The sensitivity of the responsive moiety must match the physiological concentration range of the trigger at the target stage. A ROS linker that degrades at ROS levels far below or above those actually present in the acute lesion will either fire prematurely or never fire; likewise, an MMP-cleavable sequence must be tuned to the MMP levels characteristic of the subacute-to-chronic transition [13]. Mismatched thresholds are a frequent, under-appreciated source of failure, especially given the microenvironmental heterogeneity discussed in Section 7.

Release kinetics. The rate of payload release must match the duration of the therapeutic window. Acute neuroprotective agents must be delivered rapidly (hours), whereas regenerative growth factors require sustained release over days to weeks [21, 22]. Kinetics are governed by crosslinking density, the choice of linker chemistry, and the use of reservoir structures such as PLGA microspheres or nanoparticle carriers [22].

Degradation window. The hydrogel's own lifetime must coincide with the repair timeline. Degradation that is too rapid loses the scaffold's structural support and prematurely exhausts the payload; degradation that is too slow leaves a foreign body that may itself impede regeneration. The mechanical and conductive properties of the material—ideally matched to native spinal cord, as demonstrated in the PVA/TSPBA system [21]—must also be maintained over this window, since matrix stiffness, topography, and conductivity are not passive properties but instructive physical cues that steer neural-stem-cell fate and neurite outgrowth [85].

Taken together, these three parameters constitute the "knobs" of temporal programming: by tuning threshold, kinetics, and degradation together, a designer can in principle place a given therapeutic action at the correct point on the pathological timeline. In the next section (Section 5), we map how these design principles have been applied across the four core therapeutic mechanisms.

These parameters are not free variables: the values reported by the systems surveyed here define the ranges in which they actually operate (Fig. 4). Triggers are exercised at H_2O_2 concentrations of 100–250 μM in cell and release experiments—100 μM in [21] and [32], 250 μM in [8], 200 μM in [25]—and at 2–5 mM in degradation and scavenging assays ([21] 2 mM; [8] 5 mM), one to two orders of magnitude above the former. Across the seven systems for which release data are published, the payload released first reaches half of its cumulative release between 0.4 and 6.1 days, whereas the slower payload reaches half release between 4.5 and 20 days (Fig. 5). Scaffold lifetimes measured under oxidative conditions span 20 to 24 days ([86] 20 d; [25] 24 d), against a scar that matures over 8 to 12 weeks.

Condition (c) can therefore be made quantitative without any new measurement. Each t½ is obtained by linear interpolation between the two sampling points that bracket 50% of cumulative release (all seven systems reach at least 50% for both payloads; a system plateauing below 50% would score zero by definition, since its payload never reaches the target window in effective quantity), using only the time points published in the panel cited in the Fig. 5 legend; no curve fitting or extrapolation is involved, so any value can be recomputed by hand from the original figure. Taking the half-release time t½ of each payload as its timing coordinate, and the midpoint of its designated window in Section 3 as the target, a system is temporally matched when each t½ falls inside the window of the event it is meant to serve; the separation between a system's two payloads, Δt½, measures how far apart in time its two events actually fall. Across the seven systems, Δt½ ranges from 1.4 days ([15], whose two payloads are released within five days of each other) to 14.8 days ([86], whose NT-3 reaches half release only at day 20). In two of the seven Δt½ is below six days—shorter than any single pathological stage—so their two events are effectively simultaneous, and one system ([86]) separates its two payloads by more than two weeks.

From a single payload to a program. Because τ compares one payload with one window, it extends to a whole design. Each payload is assigned the window in which its molecular target is actually active—not the window that its authors' wording implies—and its temporal match is $1 - |\log(t½/t_mid)|/\log W$, where t_mid is the geometric midpoint of that window. Averaging over a program's payloads gives a single score, the temporal matching index (TMI), which equals unity when release coincides with the centre of the target window, 0.5 at either boundary of that window, and zero once release falls outside it by a factor equal to the window's width. Scores are truncated to the interval [0, 1], so a payload released more than one window-width from the midpoint scores exactly zero. Table 2 reports the index for the seven systems with published release data. Only two exceed 0.6 (4DMSH 0.79, SilMA 0.61); five fall below, and three payloads score at or below 0.01 because they are released largely outside the period in which their target acts—paclitaxel, an anti-scar agent, is half released by day 3 against a chronic window, while minocycline and metformin, both acting on macrophage polarization, are half released within two days against a subacute one. The pattern is not idiosyncratic to individual papers but to a practice of timing release against the injury rather than against the process it is meant to address. The ranking is insensitive in its extremes: widening or narrowing every window boundary by 20% leaves the same three systems at the top and the same two at the bottom, changes no score by more than 0.16 from baseline — the largest swing across the two scenarios is DSDH, from 0.13 to 0.37, a range of 0.24 — and exchanges only the fourth and fifth places; the number of systems above 0.6 varies between one and two across these perturbations. Window assignment is a separate judgement from window width: a payload whose molecular target spans the acute and subacute intervals — several immune modulators among them — is assigned to the later of the two, which is not conservative in every case: for an inhibitor of an early innate pathway the earlier assignment is arguably the more natural one, and moving H-151 from the subacute to the acute window would lower the Sr-Zn system score from 0.44 to about 0.2 because its release begins after the acute window has closed. The same test in the opposite direction: assigning rapamycin to the subacute rather than the chronic window would raise the same system to 0.90 and make it the highest-scoring entry in Table 2, so for this system the ranking is assignment-dependent in both directions. The bottom of the table is the region most sensitive to assignment rather than to window width: moving minocycline and metformin from the subacute to the acute window would raise DSDH from 0.21 to about 0.55 and RA@Lip from 0.06 to about 0.54, and would leave one rather than three payloads released entirely outside the period in which their target acts. Window assignment, not window width, is therefore the dominant judgement in this index, and every assignment is listed payload by payload in Supplementary Table S2 so that a reader who disagrees can recompute. The choice is

therefore stated per payload rather than defended in general, and Supplementary Table S2 records it payload by payload. Supplementary Table S3 perturbs the window boundaries only; it does not re-assign payloads between windows.

Table 2. Temporal matching index for the seven systems with published release data. Windows are assigned by the period in which each payload's molecular target is active (Section 3): acute 1–72 h, subacute 72 h to 14 days, chronic 14 days to 12 weeks (Section 3.5); t_mid is the geometric midpoint of each window and W its width expressed as a ratio. Cell scores are displayed to two decimals from unrounded interpolations, and each system's score is the mean of its unrounded payload scores, so a displayed cell need not reproduce the mean exactly at the second decimal. The half-release time is read by linear interpolation between two sampled points, so its precision is set by the sampling interval; re-reading both bracketing points by ± 2 percentage points moves any single score by at most 0.05 and any system mean by at most 0.04, and the two systems at or above 0.6 remain at or above it. Scores are therefore reported to two decimals as a reading of the published curve, not as a measurement with that precision. Each system's score is the mean over its payloads.

What the index does not yet do. The index measures the distance between a design and a clock; it says nothing on its own about whether that distance matters clinically, and this review does not test that link. Nor is t½ an in vivo quantity. Every value is read from a release curve in buffer or enzyme solution, whereas in the injured cord the same material will usually release faster, because enzymatic degradation and fluid shear shorten the effective path between the payload and the tissue. The index therefore scores the timing a design intends, not the timing the tissue receives; converting one into the other requires a measurement in the lesion, and no study in this corpus reports one. The material for such a test exists but is not commensurable: Table 3 records the outcome of each system, yet the endpoints are heterogeneous — locomotor scores, cavity volume, scar area, bladder function, histological counts — measured at different times in different models, so at n = 7 no correlation can be estimated and none is reported here. A qualitative reading is still informative in one respect: the three systems with the highest index (0.79, 0.61, 0.44) all report motor or multi-modal functional recovery, while the lowest (0.06) reports a cellular readout, M2 polarization, without a functional endpoint. That pattern is consistent with the index describing design intent rather than efficacy, but it is equally consistent with reporting practice, and it is not evidence for either. The test that would settle it is a dose–response experiment in which one material is held constant and only the linker is varied, so that t½ crosses one window width while everything else is fixed; the framework predicts an optimum at the crossing and would be falsified if the outcome were flat.

Why an index rather than a label. The mismatch is not a failure of any single paper but a consequence of how the problem was posed: release was timed against the injury as the zero point, rather than against the process the payload is meant to interrupt. A label—sequential, dual-phase, cascade—records an intention, and an intention cannot be scored. An index can: it turns “is this well designed?” into a number that can be verified against a published curve, compared across systems, and used prospectively by a designer who knows the target window and must choose a half-release time. On that measure, the field's problem is not that its materials fail to release in sequence, but that the sequence they achieve is not the one the pathology asks for. Misalignment is not ineffectiveness: a payload released outside the period of peak target activity can still act, if given at a higher dose, if its therapeutic window is broad, or if its downstream effect outlasts its release. What the index measures is the loss of design margin-the further a payload sits from the centre of its window, the smaller the fraction of its dose reaching the intended target and the less room to absorb variation in injury severity, surgical timing and patient. Two limitations of the index should be stated. The index is τ on a bounded scale: 1 at the window midpoint, 0 when t½ sits a factor of W from it. It is sensitive to how the window boundaries are drawn; we tested this by widening and narrowing every boundary by 20%, and although individual scores moved by as much as 0.16 from baseline, the three highest and two lowest systems did not change places (Supplementary Table S3). And the window assigned to a payload is the period in which its molecular target is active, whereas for payloads whose effect outlasts their target — anti-inflammatory agents with downstream consequences, for instance — the effective window may be considerably wider than the molecular one, in which case the index understates their match. The windows themselves, with the molecular target and activity period behind each assignment, are listed payload by payload in **Supplementary Table S2**, and the digitised values from which every half-time was derived are in **Supplementary Table S4**. The index is therefore best read as a lower bound on

misalignment rather than as a verdict on design quality. The per-system mean scores plotted as bars, with the individual payload scores behind them, are given in **Supplementary Fig. S2**.

The index can also be read forwards rather than backwards. Figure 6 sets the same relation out as a nomogram: in each of the first three panels the two branches of every contour mark the half-release times that would give a chosen match at a given window width, so a designer who knows the target window can read off directly what t½ the material has to achieve. The fourth panel places the fourteen measured payloads in that space, and makes visible what a score alone conceals - most systems sit between the 0.4 and 0.8 contours, and the ones that miss do so by a margin the nomogram makes explicit.

System	TMI	Payload	Window	Window bounds (d)	t½ (d)	Score
4DMSH	0.79	HCT	subacute	3–14	5.3	0.87
		NT-3	chronic	14–84	20.1	0.70
SilMA	0.61	Ang-(1–7)	subacute	3–14	4.5	0.76
		NT-3	chronic	14–84	13.2	0.47
Sr-Zn	0.44	H-151	subacute	3–14	8.3	0.84
		Rapamycin	chronic	14–84	6.1	0.03
HAMA/dECM	0.43	Edaravone	acute	0.04–3	4.5	0.40
		5-HT	chronic	14–84	13.0	0.46
BSA	0.40	PTX	chronic	14–84	3.1	0.00
		bFGF	subacute	3–14	4.8	0.80
DSDH	0.21	Minocycline	subacute	3–14	1.4	0.00
		IL-4	chronic	14–84	12.0	0.41
RA@Lip	0.06	Metformin	subacute	3–14	0.4	0.00
		Retinoic acid	chronic	14–84	7.0	0.11

5. Temporal modulation of the four core pathological mechanisms

The design principles of Section 4 map onto four core therapeutic mechanisms, and in each case temporal matching—rather than mere responsiveness—determines outcome. Each subsection follows the same logic: the mechanism (recalling Section 3), the design strategy, and representative systems.

5.1 Inflammation and immunomodulation: programming the M1→M2 switch

Inflammation is a temporally ambivalent force in SCI: early inflammation is necessary for debris clearance, but its persistence drives secondary damage (Section 3.2). The therapeutic goal is therefore not wholesale immune suppression, but the temporal reprogramming of the immune response—skewing the balance from a pro-inflammatory M1 toward an anti-inflammatory, pro-regenerative M2 phenotype, and doing so at the right time [42, 46].

Before surveying how hydrogels pursue this goal, one caveat governs the language of this section. The M1/M2 dichotomy is an *in vitro* construct that poorly captures the *in vivo* reality of myeloid cells, which exist on a continuous spectrum [47]; single-cell work has since resolved the compartment into subpopulations-including disease-associated microglia that

persist for months and contribute to recovery-whose transcriptomes map onto neither pole [50, 51, 88]. The therapeutic target is therefore not a switch between two poles but the steering of disease-associated transcriptional programs along the injury timeline, driven by NF-kB, STAT1 and IRF on one side and STAT6, PPARγ and PI3K/Akt on the other [89, 90]. The immunopharmacological application of these switches to spinal cord injury is set out in [91]. We retain the M1/M2 vocabulary, flagged as such, because it is the currency in which the reviewed studies report results; every M1-to-M2 claim should be read as a coarse proxy for a shift toward the reparative end of the spectrum [91].

Passive immunomodulation. A classic, non-responsive strategy is exemplified by the DAMP-scavenging, IL-10-releasing hydrogel, in which a cationic polymer (polyamidoamine) continuously binds anionic DAMPs while IL-10 is slowly released; in a complete transection model this dual-functional scaffold suppresses pro-inflammatory cytokines, promotes the M2 phenotype, and achieves scar-free axonal regeneration [11]. This system acts continuously rather than responsively, and thus illustrates the contrast that motivates temporal programming: it addresses “what to remove” (DAMPs) rather than “when to intervene.”

Temporally programmed immunomodulation. SilMA illustrates the consequence: rapid release of angiotensin-(1–7) induces M2 microglial polarization early (1.8-fold), and the later, sustained release of neurotrophin-3 shifts the system toward neural differentiation (3.6-fold), reducing astrocyte scarring by 54% [22] (Fig. 7). Its genuine achievement is a temporal *hand-off*—the anti-inflammatory signal is delivered when inflammation peaks and is then superseded by a regenerative signal, something a continuous anti-inflammatory scaffold cannot do.

However, its temporal order is engineered, not sensed, and this distinction carries concrete limitations. The sequence of Ang-(1–7)-then-NT-3 arises from *differential release rates*, not from any responsive trigger: both payloads are released on pre-set, open-loop kinetic schedules. The system does not “know” when inflammation has resolved; it merely assumes that by the time NT-3 predominates, the inflammatory phase will have passed. It is therefore a *scheduled* program rather than a *gated* one—order is imposed by the clock of the material, not by the state of the pathology (Section 4.2 distinguishes these two routes explicitly). Because NT-3 release is decoupled from inflammation sensing, a lesion in which inflammation persists longer than expected will receive a regenerative signal while the microenvironment is still hostile, attenuating its effect; conversely, a lesion that resolves inflammation rapidly will have already transitioned to regeneration before the kinetic schedule delivers NT-3, wasting the early regenerative window. Both are realistic given the microenvironmental heterogeneity discussed in Section 7. Relative to Level III, the system lacks response-based gating (its second event is not triggered by a pathological cue) and any feedback loop; it satisfies the *encoding* and *ordering* criteria of the time-programmable definition, but only weakly satisfies *temporal matching*, since its timing is asserted rather than verified against the pathology. It is, in effect, a two-event sequence with an open-loop timer—one step removed from a genuinely pathology-gated program.

A third system—the dual-drug sequential-delivery hydrogel (DSDH)—represents a meaningful step *toward* genuine gating within the immunomodulatory axis, and thus a useful counterpoint to the SilMA's open-loop kinetics. DSDH couples a hyaluronic-acid matrix with fucoidan nanoparticles to release minocycline in the early acute window (suppressing M1 polarization) and, crucially, a **biotin–streptavidin affinity system** to withhold interleukin-4 until the late, non-acute stage, where it promotes M2 polarization [87]. The biotin–streptavidin interaction is the point of distinction: unlike the SilMA's passive release-rate difference, it imposes a *physical affinity barrier* that must be overcome before IL-4 is liberated, so the second event is not merely slower but actively *retained* until its designated window. In a rat contusion model, DSDH programmatically shifted the inflammatory microenvironment—reducing scar formation, improving motor function and bladder control, and shrinking the lesion cavity—relative to a non-sequential dual-drug control [87]. **What it achieves**, then, is a genuine *ordering mechanism* (affinity-gated, not merely rate-scheduled) within the immunomodulatory stage. Its gating is *kinetic/affinity-based*, not *pathology-sensing*—IL-4 release is delayed by design, not triggered by a measurable resolution of inflammation—and it spans only the inflammatory→regenerative transition, remaining a two-event, single-axis program with no feedback. Relative to Level III, DSDH narrows the gap in the *ordering* dimension but still lacks pathology-coupled gating, a third mechanism (or stage), and closure. Beyond these staged systems, the single-response immunomodulatory toolkit

continues to broaden: injectable, self-healing hydrogels integrating curcumin with quaternized chitosan and polydopamine remodel the immune microenvironment through ROS scavenging and M2 polarization, with glial-scar inhibition emerging as a downstream consequence rather than a directly targeted endpoint [92].

5.2 Oxidative stress and ROS: temporal ROS scavenging and nanozyme strategies

Oxidative stress is the dominant acute-phase insult, and ROS is both the pathology and—crucially—the endogenous trigger (Section 3.1). This dual role makes ROS the ideal first step in any cascade: a hydrogel that senses ROS can simultaneously neutralize it and use it as a gate for subsequent responses [8, 9]. The underlying chemistry is now mature: ROS-cleavable linkers (thioketal, arylboronic ester, phenylboronic acid ester) and ROS-scavenging nanomaterial payloads constitute a well-established toolkit whose sensitivity thresholds and degradation profiles can be rationally tuned to the oxidative microenvironment [93].

Nanozyme-mediated ROS scavenging. A family of antioxidant nanozymes—MnO_2, nanoselenium, and ZnO-based metal-organic frameworks—forms the material backbone of this strategy. The nanoselenium nanozyme hydrogel clears ROS, upregulates antioxidant enzymes, reduces caspase-3-dependent apoptosis, and promotes regeneration [8]. The ZnO-ZIF8 nanozyme hydrogel couples NIR photothermal effects with pH-triggered Zn^{2+} release to upregulate GPX4 and HO-1, thereby inhibiting ferroptosis—an iron-dependent, lipid-peroxidation-driven cell death that has emerged as a distinct oxidative-injury mechanism in SCI [9, 94, 95]. A further refinement targets ROS at its mitochondrial source: the one-step PLCS hydrogel preferentially releases the mitochondria-directed peptide SS31 before lipoic acid sustains cytosolic clearance, while supplying choline and acetyl-CoA for cholinergic-neuron maturation [25]. The breadth of this acute-phase strategy is now considerable, spanning ferroptosis suppression through the Nrf2/Slc7a11/GPX4 axis [96–100], in which GPX4 induction and lipid-peroxidative death recur as the mechanistic focus; stem-cell combination and macrophage-polarization steering [101–103]; and mitochondrial-ROS targeting [26, 92, 104, 105] — a redundancy that motivates the field's shift toward temporal sequencing.

ROS as the first step of a cascade. The ROS→MMP hydrogel is the field's clearest realization of a *gated* two-step program, and it demonstrates what sequential encoding can achieve: ROS-triggered release of ROS-scavenging nanodrugs (CNT@MnO_2) provides acute neuroprotection, and only later does MMP accumulation release VEGF for angiogenesis and neural stem cell differentiation [21] (Fig. 8). The ROS signal thus serves as the “clock” that times the acute intervention, with the MMP signal gating the later regenerative step—a genuine logical dependency between events, not merely coexistence.

The cascade is also narrower than its framing suggests. Only the first gate is quantified in the main figures: network breakdown under H_2O_2 releases the ROS-scavenging nanodrug, and the loss of matrix mass tracks that opening (Fig. 8). The second gate is evidenced through its downstream consequence—angiogenesis and neuronal differentiation attributed to MMP-liberated VEGF—rather than through a released-VEGF curve, which is not reported in the main text [21]. In our assessment, the field's most complete cascade rests on a single directly quantified trigger, while the second transition is demonstrated by its effect rather than by its kinetics. Condition (c) asks whether the timing can be verified from release data, not whether the original study chose to verify it; a gate whose opening is inferred only from a downstream effect therefore satisfies (a) and (b) fully and (c) only in part, and we score it accordingly.

Yet this system is instructive as much for what it *omits* as for what it achieves, when read against the pathological timeline of Section 3. Its two events map onto the acute (ROS) and subacute-to-chronic transition (MMP) stages, but it bypasses the subacute inflammatory peak entirely: no event is dedicated to immunomodulation, so the M1-polarized environment that dominates the days-to-weeks window is left to resolve spontaneously rather than being actively steered (Section 3.2). The program therefore “jumps” from neuroprotection to regeneration across an un-addressed inflammatory middle. The design depends on ROS remaining available as a trigger long enough to gate the first event, yet its very payload—CNT@MnO_2—is a potent ROS scavenger: over-efficient scavenging can depress the very signal that the cascade relies on, effectively choking the gate it is meant to open. Conversely, if MMP expression is delayed or attenuated in a given lesion (as in milder or slower-

evolving injuries), the second event may fire late or weakly, decoupling regeneration from its intended window. Relative to Level III, the system lacks at least two capabilities: a third event (an immunomodulatory step inserted between neuroprotection and regeneration), and any feedback sensing—it is a fixed, open-loop sequence of two pre-set triggers with no capacity to detect when one stage has actually resolved before advancing. It is, in short, a genuine two-step cascade, but one that remains two steps short of a closed-loop, ≥ 3-mechanism program.

5.3 Glial scarring and microenvironment remodeling: the least-covered chronic stage

Glial scarring is the chronic-phase barrier that most directly prevents axonal regeneration [2] (Section 3.3), yet—as established in Sections 2.4 and 4.3—the only staged program designed to terminate here does not arrive in time: its scar-directed payload is half released on day 3, before the chronic window opens. With that program discounted, the remaining chronic-phase work consists of isolated, single-step interventions rather than the terminal event of a sequence. This gap is both a challenge and an opportunity, and recent work is beginning to close it. The scar is increasingly appreciated not as a monolithic barrier but as a dynamically organized, multicellular structure whose molecular landscape and cellular crosstalk shift across the acute-to-chronic transition [106–108]; mechanoregulation of scar-forming fibroblast patterning ($Il11ra1^{+}$/$Itga11^{+}$) [109] and scar-homing delivery strategies [110] exemplify this more refined, mechanistically informed view. Against this backdrop, the scar's dual nature—protective early, inhibitory late—defines the precise temporal constraint that any anti-scar intervention must respect (Section 3.3).

Molecularly targeted scar inhibition. Two emerging targets exemplify the shift from structural to molecular scar modulation, and—read critically—together expose the unresolved tension between anti-scar efficacy and the scar's protective functions.

The N-cadherin nano-antagonist hydrogel inhibits the aggregation of scar-forming astrocytes by antagonizing the integrin–N-cadherin pathway, impeding glial scarring and promoting axonal regeneration [14]. **What it achieves** is a genuinely mechanistic intervention: it disrupts a specific molecular driver of scar *compaction*. Its temporal logic is a single, open-ended suppression with no stage specificity—it does not distinguish the early, protective phase of reactive astrogliosis from the later, growth-blocking consolidation of the mature scar. This is a defined **failure mode with a concrete cost**: N-cadherin-mediated aggregation is precisely what, in the subacute window, walls off the lesion and confines cytotoxic inflammation to protect spared tissue [59]. A stage-blind antagonist that suppresses this aggregation from the outset therefore weakens the very barrier whose early formation prevents secondary injury expansion, converting tissue that would have survived into secondary loss. One might counter that early immunomodulation (Section 5.1) should subdue the inflammatory storm and render the scar's protective role dispensable. The objection is correct in *logic* but not in *conclusion*: it argues *for gating* scar inhibition *behind* immunomodulation, not for timing-blind suppression—immunomodulation acts gradually, and during the transition window the early protective barrier is still needed. The correct design is therefore a *sequence*—an anti-scar event released only after the upstream immune program has actually softened the environment—precisely the pathology-coupled gating that an unconditional N-cadherin antagonist cannot sense. The system's real defect is not that it inhibits the scar, but that it does so *unconditionally*: relative to Level III, it is a single-stage, single-target intervention lacking ordering, gating, and feedback—the absence of *timing* that converts its efficacy into a liability.

The thermoresponsive ATRA-loaded hydrogel targets Pin1, a peptidyl-prolyl isomerase that drives astrocyte proliferation and scar formation through the PI3K/AKT/CDK2 axis; sustained ATRA release suppresses Pin1 [16] (Fig. 9). The thermoresponsive vehicle solves ATRA's short half-life through sustained release, adding temporal control to a molecular anti-scar strategy. As with N-cadherin, Pin1 inhibition is a single, stage-blind suppression; but its failure mode follows from the *identity* of its target rather than its delivery. Pin1 regulates the PI3K/AKT/CDK2 axis, which also sustains the survival and homeostatic turnover of neurons and glia in spared tissue—so sustained suppression carries an **off-target cost**: even with local retention, the molecular reach of Pin1 blockade exceeds the lesion boundary. It also carries the same **timing cost** through a different mechanism: the earliest astroglial response is protective, and an open-ended Pin1 blockade cannot be withdrawn once the scar has matured and its suppression is no longer beneficial. Its “temporal control” is therefore a

delivery property, not a *programmed sequence*: there is no gated second event and no release of the brake once the protective-to-inhibitory transition has passed. Relative to Level III, it is a single-step intervention with a delivery improvement, not a cascade—it occupies the chronic stage in isolation, exactly the field's central gap.

Enzymatic degradation of the scar matrix. A complementary chronic-stage route attacks the scar not at its *formation drivers* (N-cadherin, Pin1) but at its *deposited matrix*—the chondroitin sulfate proteoglycans (CSPGs) that form its inhibitory core. Two systems illustrate the strategy. A chondroitinase ABC-immobilized nanoclay hydrogel (ChABC@Lap) electrostatically immobilizes the enzyme inside Laponite nanoclay; the injectable, shear-thinning gel suppresses pro-inflammatory macrophage activation and degrades CSPG, lowering GFAP and CS-56 deposition and improving recovery [111]. A second identifies CSPGs as regulators of scar *maturation* through a pathogenic microglia–astrocyte axis, in which CSPGs suppress microglial cytochrome P450 (CYP450) activity to sustain a pro-inflammatory state; a ROS-responsive, CTGF-binding lipopolyplex then delivers the ChABC *gene* for targeted CSPG degradation at the lesion border [112]. Both couple the enzyme to stabilizing vehicles to overcome ChABC's thermal instability, a strategy now systematized across carriers [113]. Unlike the N-cadherin/Pin1 targets, they intervene on the *substrate*, and [112] couples the intervention to a pathological trigger (ROS) and a mechanism (CSPG→CYP450 crosstalk)—a step toward pathology-coupled anti-scar strategy. Neither is gated into a multi-step sequence, and this carries a timing-dependent cost directly analogous to the N-cadherin/Pin1 failures, transposed from the scar's *formation* to its *degradation*: CSPGs are deposited within 24 h and serve protective/guidance roles before the inhibitory scar consolidates [55], so a continuous single-step ChABC treatment degrades CSPG indiscriminately across the timeline—unable to withhold degradation during the early protective window or to concentrate it on the later inhibitory phase. This is why ChABC monotherapy has produced variable outcomes: enzymatic degradation is effective only when it coincides with the moment an axon is ready to traverse the lesion, and a timing-blind enzyme spends its finite activity on the wrong phase. Relative to Level III, these systems narrow the gap on *mechanism* and *trigger* while leaving *multi-step ordering* open. An immunomodulatory microneedle patch (Z@C-MN) extends the arsenal by coupling pH-gated ChABC/Zn^{2+} release to $CD4^+$ T-cell modulation [114], yet it too remains a single intervention rather than a gated node within a cascade. Adjacent chronic-stage strategies—pH-responsive minocycline depots curbing M1 polarization at the scar border [115], and thermo-sensitive depots delivering engineered exosomes to reprogram glial reactivity [116]—likewise address the scar as a single stage rather than a gated node within a sequence.

Scar modulation within a temporal program. In our view the most compelling recent development is the integration of scar inhibition into a staged sequence. The dual-phase SilMA hydrogel reduces astrocyte scarring by 54% as a *consequence* of its early M2 polarization and later neuronal differentiation [22]; similarly, the BSA hydrogel's dual release of paclitaxel (anti-scar) and bFGF (pro-regeneration) addresses scar inhibition and axonal regrowth within a single two-event program [15]. These examples point toward a future in which the chronic-phase scar—currently the weakest link—is addressed not in isolation but as the intermediate step of a multi-stage cascade (Section 7).

5.4 Axonal regeneration and myelination: the regenerative endpoint

The ultimate goal of all temporal programming is the restoration of neural connectivity—axonal regeneration, neuronal differentiation, and remyelination (Section 3.4). Here the temporal constraint is decisive: regenerative signals are effective only after the acute inflammatory storm has subsided, so premature delivery is wasted and appropriately timed delivery is essential [62]. Remyelination, in particular, is a slow and often incomplete process: endogenous oligodendrocyte progenitor cells (OPCs) proliferate and differentiate for months after injury, yet the resulting myelin repair rarely keeps pace with demyelination, leaving surviving axons chronically denuded and functionally compromised [117, 118].

Growth-factor and neurotrophin delivery. The dual-phase SilMA system's sustained NT-3 release drives neural stem cell differentiation into neurons (3.6-fold) and reduces astrocyte differentiation, embodying the late regenerative signal of a staged program [22]; it is this late phase that the reduced astrocyte scarring reported in Section 5.3 ultimately reflects. The ROS→MMP hydrogel's MMP-gated VEGF release similarly provides the late pro-angiogenic and pro-differentiation signal [21]. These systems converge on a shared design logic: neurotrophic and angiogenic factors belong at the *end* of the

temporal sequence. This logic echoes a broader consensus in cell-based SCI repair, where the delivery of neurotrophic factors (NT-3, BDNF, GDNF) and the steering of neural stem/progenitor cell fate—away from the astroglial default and toward neuronal and oligodendroglial lineages—are recognized as the decisive determinants of whether transplanted or endogenous precursors contribute to circuit repair rather than to scar [119, 120]. A recent realization couples this fate-steering to a sustained-release scaffold: an engineered exosome displaying a GDNF/NT-3/IGF-1 cocktail, delivered within an ionic-liquid-modified cellulose-nanocrystal/silk-fibroin hydrogel, simultaneously remodels the inflammatory niche and redirects endogenous neural stem cells away from astroglial differentiation and toward neuronal and oligodendroglial lineages through parallel PI3K–AKT and Wnt/Ca^{2+} modules [121].

An exogenous clock for temporal control. A complementary route to timing the regenerative signal is provided by exogenous-stimulus scaffolds, which place the “clock” in the clinician's hands rather than in the pathology. Conductive nanocomposite hydrogels and magneto-electric Fe_3O_4@$BaTiO_3$ composites generate electrical stimulation—remotely and non-invasively in the latter case—that promotes neuronal differentiation and axonal growth on a scheduled, on-demand basis [7, 20]. The conductive route has since been extended in two directions: a phenylboronic-acid/dopamine/MXene scaffold whose modulus and conductivity match native cord tissue couples electrical stimulation with M2 polarization and endogenous neural-stem-cell neuronal differentiation [122], and a carbon-nanotube/gelatin conductive hydrogel paired with external electroacupuncture reconstructs the electrochemical niche to attenuate inflammation, reduce glial scarring, and promote axonal regeneration and remyelination while improving both motor and bladder function [123]. These systems do not change the underlying design principle but rather its implementation: where endogenous triggers rely on the fidelity of the pathological signal, exogenous stimulation offers precise, externally controlled timing at the cost of requiring instrumentation. Both routes converge on the same conclusion—regenerative signals must arrive late, after inflammation subsides—and their relative merits for translation are discussed in Section 7.

6. State of the art: recent representative systems

The preceding sections established the design principles and their application across the four core mechanisms. Figure 1 distinguishes seven response chemistries; for clarity this section groups them into six chemical families — ROS, pH, enzyme, temperature, magnetic/electrical and photo/NIR — and treats systems with no chemical trigger separately, because their ordering is architectural rather than chemical. Cascade-and-sequential logic is likewise an architecture, not a chemistry, and is discussed below. Table 3 presents a representative subset of the 57 systems, ordered by their position on the single-response to cascade continuum; the complete roster, organized by response modality, temporal level, pathological stage and primary endpoint, is given in **Supplementary Table S1**. Two distributional patterns emerge from this roster. First, single-response systems dominate: ROS-scavenging, enzyme-, pH-, temperature-, photo-, and conductive/magneto-electric platforms are individually abundant but, by definition, engage only one point in the pathological timeline [8, 9, 13, 16, 18, 30, 124–132]. Second, the field is in active transition toward dual-phase and cascade strategies (Level II), which remain a minority—while multi-step cascades that span three or more distinct pathological stages or mechanisms (Level III) remain unrepresented. The underlying material principles—substrate design, network architecture, degradation behaviour, conductive and multimodal integration—have been systematized across recent reviews of bioactive-hydrogel design, MMP- and thermosensitive platforms, conductive and smart-responsive materials for neural repair [74, 133–137].

ROS- and antioxidant-responsive systems (n = 17). These form the largest chemical class, and their dominance is easy to explain: the acute lesion supplies the highest-amplitude, most sharply time-locked trigger on the timeline. Their limitation is structural rather than technical. Because each responds to the same cue and acts once, they occupy a single point in time, and the redundancy documented in Section 5.2—nanozymes, ferroptosis inhibitors, mitochondrial scavengers—improves potency without extending temporal coverage.

Enzyme-responsive systems (n = 4). MMP- and hyaluronidase-cleavable platforms answer signals that rise after the acute burst, which makes them the natural second step of a cascade; in practice almost all are deployed as single-response carriers of a growth factor, so the temporal advantage is left unused.

pH- and temperature-responsive systems (n = 3 and n = 3). These behave less as therapeutic triggers than as delivery hardware. Acid-labile carriers release their cargo where the tissue is already acidic, and thermoresponsive gels provide an in situ depot; both support a payload rather than impose an order on it.

Magnetic, electrical and photonic systems (n = 10 and n = 2). These place the clock in the operator's hands. Remote stimulation can be switched on at any chosen moment, decoupling timing from the fidelity of the endogenous signal—the central weakness of the triggers above. The cost is instrumentation and, for photothermal systems, heat delivered to tissue that is already injured.

Systems with no chemical trigger (n = 18). The largest single category is defined by what it lacks. These systems order their payloads by architecture—a core-shell geometry, an electrostatic barrier, a differential diffusion path—rather than by a cue from the lesion, and they account for eleven of the thirteen Level II systems discussed below. Their existence is the strongest single argument of this review: the field is already building sequences, but it is building them on the material's clock.

Dual-phase and cascade systems are the clearest embodiment of the time-programmable principle and, in our view, the most significant recent development. Both routes are shown in Fig. 5. That this route is actively expanding, rather than remaining an isolated demonstration, is underscored by the subsequent time-specific four-dimensional SilMA hydrogel (4DMSH) from the same group [86]: it likewise programs a sequential hand-off—rapid Houttuynia cordata extract for early anti-inflammatory action, followed by sustained NT-3 for late neuronal differentiation—and extends the concept to motor, sensory, and autonomic recovery.

The pace of this expansion has accelerated further in 2026. The RA@Lip/Met-HSB liposome–zwitterionic nano-hydrogel releases metformin in the acute phase to polarize microglia toward M2 while electrostatically retaining retinoic-acid-loaded liposomes for the chronic phase, when retinoic acid drives neural stem cells toward GABAergic neurons and oligodendrocytes [138]; and the edaravone/serotonin dual-drug biomimetic hydrogel (HAMA/dECM) delivers edaravone acutely to suppress microglial pyroptosis via the NF-κB–NLRP3–caspase-1–GSDMD axis before sustained serotonin release supports chronic axonal regeneration and remyelination [139]. Extending the sequential logic from the innate to the adaptive immune axis, an Sr-Zn mesoporous bioactive-glass platform stages three temporally ordered events—early STING-inhibitor (H-151) release to suppress cGAS–STING signaling, subsequent rapamycin release to drive regulatory T-cell (Treg) differentiation via mTOR inhibition, and CCL22-mimetic peptide-mediated Treg recruitment—so that acute innate suppression hands off to sustained adaptive tolerance while Sr^{2+}/Zn^{2+} ions support neural remodeling; Treg depletion or CCR4 blockade abrogates the benefit, confirming the adaptive arm's causal role [32].

These newest additions confirm that staged delivery—once a single demonstration—is now an established, rapidly growing design class.

Yet the staging in [32] is less than it appears: its three events are released by a single ROS trigger — a shared cue, so that none of them is ordered by a distinct chemistry — with H-151 and rapamycin following near-parallel profiles that differ by only 10–17 percentage points; measured against the target window, moreover, H-151 — nominally the earlier of the two events — is released the more slowly (t½ 8.3 versus 6.1 days; Table 2), so the intended order is not supported by the release kinetics at all. The two observations are consistent: a near-constant vertical offset of 10–17 percentage points between two steep curves corresponds to a horizontal displacement of roughly two days, so near-parallel profiles and a two-day difference in half-release time describe the same curve from two axes. Rapamycin is nevertheless scored against the chronic window rather than the subacute one, because the adaptive arm it depends on — Treg differentiation and sustained tolerance — matures over weeks rather than days; the assignment is stated here rather than left implicit because it is consequential, and judging the same release against the subacute window would raise the system's index rather than lower it. Ordering and timing are independent axes, and this system separates them cleanly: H-151 falls inside the window it is meant to serve (score 0.84) but rapamycin does not (0.03), and the one released first is the one meant to act second — the

program is both misordered and mistimed, and the two failures are independent — a program can be well timed and wrongly ordered at the same time, and the converse is equally possible. The third element, in turn, is not released at all: CCL22 is presented on the particle surface, so what is staged is the payload rather than the trigger. Across the systems for which release data are published, the separation between the fast and slow payloads spans an order of magnitude-from roughly 15 to 78 percentage points at one week-and in every case it arises from diffusion or hydrolysis rather than from a second cue.

The breadth of this class is further evident in the parallel designs now emerging across the field: dual-responsive bilayer hydrogels [139], zwitterionic injectable nanogels [140], dual-enzyme nanofibers [141], core-shell microspheres [142], hydrogen-and-magnesium microneedle patches [143], mitochondria-targeted photothermal systems [144] and architecture-engineered electrospinning cascades [145, 146]. Their emergence signals a genuine paradigm shift from “what to deliver” to “when and in what sequence to deliver.”

A synthesis of these modalities reveals the field's trajectory: single-response systems are converging toward cascade designs, and the next logical step—multi-step cascades that span three or more distinct pathological stages or mechanisms and thereby bridge the chronic glial-scarring stage—remains unclaimed. This gap is the focus of the final section. Table 3 consolidates the representative systems discussed above, ordered by their position along the single-response → cascade continuum.

Table 3
Representative responsive and time-programmable hydrogel systems for spinal cord injury repair.

System (material + cargo)	Response mechanism	Temporal logic	Pathological stage(s)	Key outcome	Ref
PVA/TSPBA delivering CNT@MnO_2/VEGF	ROS- and MMP-cleavable	Chemical cascade (ROS → MMP)	Acute → regenerative	Structural and functional recovery at 6 weeks in two clinically relevant SCI models	[21]
SilMA delivering Ang-(1–7)/NT-3	Release kinetics	Dual-phase (rapid → sustained)	Inflammatory → regenerative	Astrocyte scarring reduced by 54%; improved motor function	[22]
DSDH (HA/fucoidan) delivering minocycline/IL-4	Biotin–streptavidin affinity gating	Gated sequential release	Inflammatory	Lesion cavity reduced to 76.6% of control; improved motor and bladder function	[87]
4DMSH (SilMA) delivering HCT/NT-3	Time-specific release	Sequential hand-off	Inflammatory → regenerative	Motor, sensory, and autonomic recovery	[86]
BSA delivering PTX/bFGF	Dual release kinetics	Dual-phase	Chronic scar + regeneration	Scar inhibition and axonal regrowth	[15]
RA@Lip/Met-HSB nano-hydrogel	Electrostatic liposome retention	Sequential (Met → RA)	Inflammatory → chronic	M2 polarization → neural differentiation (GABAergic/oligodendrocyte)	[138]
HAMA/dECM delivering edaravone/5-HT	Dual-drug sequential release	Sequential (acute → chronic)	Acute → chronic regeneration	Pyroptosis suppression → remyelination	[139]
Sr-Zn mesoporous bioactive glass (STING inhibitor/rapamycin/CCL22)	Three-stage temporal release	Three-step (innate → adaptive immune)	Inflammatory	Treg differentiation; benefit abolished by Treg depletion	[32]
N-cadherin nano-antagonist hydrogel	Molecular targeting	Single-response	Chronic (scar)	Impaired astrocyte aggregation, promoted regeneration	[14]
Thermoresponsive chitosan/β-GP delivering ATRA	Temperature-responsive	Single-response (sustained)	Chronic (scar)	Pin1 inhibition, reduced glial scarring	[16]
ChABC-immobilized nanoclay (Laponite)	Enzyme immobilization	Single-step (continuous)	Chronic (scar)	CSPG degradation + anti-inflammation	[111]
ROS-responsive CTGF-binding lipopolyplex (ChABC gene)	ROS-responsive gene delivery	Single-event	Chronic (scar)	Scar-border CSPG degradation, scar-free repair	[112]
Z@C-MN microneedle patch	pH-responsive	Single-event	Chronic (scar)	Scar inhibition + $CD4^+$ T-cell modulation	[114]

7. Challenges and future directions

Why the sequence should be carried by the material. The framework assumes that temporal order ought to be encoded in the implant, and that assumption deserves an argument rather than a premise. Four routes can deliver two agents in a fixed order: a single implant whose chemistry or architecture sets the schedule; repeated local injections; an external pump or programmable reservoir; and systemic dosing with a disease-modifying agent. Repeated injection is the simplest and is routine in oncology, but in the injured cord each pass through the dura carries infection and arachnoid-scarring risk, and the second injection must find a cord that has already been operated on. An external pump avoids re-instrumentation but

requires a tunnelled catheter and a patient or carer able to operate it for weeks, which is unrealistic for a population with a median age in the fifth decade and frequent concomitant trauma. Systemic dosing reaches the cord poorly across the blood–spinal cord barrier and exposes off-target tissue to the same agent. Material-encoded delivery wins not because it is more sophisticated but because the clinical pathway already contains one open-dural moment: decompression and duroplasty. The sequence must therefore be complete at implantation, which is exactly what an implantable clock provides and what none of the alternatives can guarantee without a second procedure. The corollary is a real constraint rather than a rhetorical one: the clock must run for weeks inside a swelling, enzymatically active, mechanically loaded lesion, and it must do so open-loop, since no external reader will adjust it. A pump can be reprogrammed; a hydrogel cannot. Any claim for material-encoded sequencing is a claim about robustness under those conditions, and the burden of proof sits with the material. The time-programmable framework faces several outstanding challenges that define the field's immediate research agenda.

Microenvironmental heterogeneity and threshold mismatch. A fundamental assumption of endogenous-trigger design is that the pathological signal is reliable and predictable; in reality the SCI microenvironment is highly heterogeneous across patients, severity, and time, so a ROS linker tuned to an “expected” level may fire too early or not at all [18]. This argues for broad, tunable response windows or for exogenous clocks to supplement unreliable endogenous signals. A related barrier is the **Model-versus-human mismatch, reformulated as a scaling problem.** The pathological timeline of rodent SCI does not map linearly onto human SCI: the acute-to-chronic transition, the kinetics of inflammation and the maturation of the glial scar all differ in timescale [2], so a program tuned to a rat contusion may be mis-timed in a patient. The difficulty becomes tractable once timing is expressed as a dimensionless ratio. Writing W for the width of a payload's target window and t½ for its half-release time, the design condition is that $\tau = t_{1/2}/W$ falls inside the range in which the payload is both present and needed. The two clocks are then explicitly different in kind: t½ is a property of the material and can be tuned, whereas W is not directly tunable by the material designer, although it can be altered by an upstream therapeutic intervention; it is not a variable the material can set. Translation reduces to a single question—how W changes between species—rather than to a diffuse appeal for validation, and answering it requires time-resolved pathology in at least two further species, sampled across the acute-to-chronic transition; endpoint histology at one late time point, which is what most large-animal studies report, cannot constrain W.

What this gap means for the present evidence base. The limitation is not abstract. The 57 included studies use rodent contusion, compression or transection models, in which injury, treatment and endpoint fall inside a single 8–12 week window; none reports a large-animal injury model, and none reports time-resolved pathology in a large animal; none measures how the width of a target window W changes with species, and none carries a hydrogel from a small animal into a large one. The clinical side is thinner still: no temporally programmed hydrogel has been tested in patients, so there is no human W against which any scaling law could be checked. This is a statement about the state of the evidence rather than a defect of the framework, but it does mean that the $t_{1/2}/W$ formulation is for now a way of specifying what must be measured, not a tool that has been validated.

The clinical clock and the research clock. Every release curve in this review is referenced to the moment of injury. Clinical implantation is not. In the two surgical series available to us, the median interval from injury to decompression was **27.8 h** (IQR 15.4–61.9; 47% within 24 h) in a Norwegian cohort and **66.9 h** (range 3-4094.6; n = 469) in a North American one, and ultra-early surgery (< 12 h) is achieved in a minority [147, 148]. By the time a material is placed, the excitotoxic phase that the earliest acute designs address is over, although the oxidative phase is not: reactive oxygen species rise over the first hours and stay elevated for several days, so an implant placed at 24–72 h lands inside that plateau rather than before it. The mismatch is therefore one of target as much as of timing: the designs are built for the fastest event, while the clinical pathway delivers them into a phase that is slower and still open. The matching condition must therefore be referenced to the residual window, with W measured from implantation rather than from injury; where that residual window is empty, no choice of t½ can recover it. Where release kinetics are fixed at manufacture, the implantation window must be chosen to fit them; where they are tunable, the window can be met. What no longer works is a program specified against a window that

has already closed. The asymmetry is starker at the other end. Chronic lesions have been implanted with scaffolds in completed clinical work [149], and a defined cavity with consolidated borders is surgically easier than a swollen, haemorrhagic acute cord. That access has a price worth naming: the clinical series that achieved it **resects the scar before implantation**, which is precisely the wholesale ablation argued against in Section 3.3. The chronic window is therefore reachable, but only by removing the structure that a temporally modulated material would be designed to keep and re-educate. Yet the chronic stage is the primary target of six of the 57 systems reviewed here and the designed terminus of one ([15], which does not reach it in time). In this sample, attention tracks design tractability rather than clinical burden, and the burden is inverted: the window that is easiest to design for is the hardest to reach, and the window that is easiest to reach is the one the field designs for least. **We call this the tractability-accessibility inversion.** In our own coding it is not subtle: 23 of the 57 studies build for the acute window, whose most sharply time-locked events — the oxidative burst and the excitotoxic cascade — peak within the first hours to a day, whereas decompression is performed at a median of 28–67 h after injury: the window is still open, but its steepest part has already passed. Only 6 build for the chronic window, the one stage that can be entered electively and the only one for which surgical precedent exists. **The field designs for the window it cannot reach in time, and under-designs the one it can enter electively.** Table 4 sets the two axes against each other.

Table 4
Design tractability and clinical accessibility by pathological stage.

Stage	Design tractability	Clinical accessibility	Systems with this primary target (n = 57)
Acute (0–72 h)	High: strongest, most time-locked trigger	Low-moderate: median 28–67 h from injury to surgery	23
Subacute (3 d-2 wk)	Moderate	Moderate: a planned second procedure is feasible	12
Chronic (2–12 wk)	Low: weak, scar-dominated signalling	High: stable cavity; clinical implants exist	6
Regenerative (overlapping)	Moderate	Moderate	16

Timing and mechanics remain confounded. Scanning τ to locate an optimum presupposes a platform in which t½ can be varied while everything else is held constant. In most hydrogels it cannot: crosslink density sets release rate and modulus together, and modulus alone alters astrocyte reactivity and axon growth. A difference observed between two release schedules may therefore reflect the mechanical change that accompanied it rather than the timing. Until a platform decouples the two—by fixing modulus and varying only the linker chemistry, or by orthogonal crosslinking—the window-scanning experiment the framework calls for cannot be interpreted. The decisive experiment follows directly from this: a platform that fixes modulus and varies only linker chemistry, producing half-release times spanning roughly one window width either side of unity, tested in a single injury model, would yield a dose-response curve of functional recovery against τ. That curve would either confirm the framework's central prediction or falsify it, and no study in the set has produced one. The objection limits what a retrospective comparison can establish; it does not make the framework untestable. Decoupling is an engineering problem with known solutions-fixing modulus while varying only the linker, or building orthogonal crosslinks-and once it is solved the τ formulation becomes falsifiable in the ordinary sense: it predicts an optimum that a given system can be shown to miss.

The chronic-stage gap: a mechanistic diagnosis. The bibliometric distribution (Section 2.4) renders this gap visible: one two-event program is designed to terminate in the chronic glial-scarring stage, and it discharges its scar-directed payload by day 3, well before that window opens (Table 2); no other curated system addresses the stage as its final event—but a structural observation alone does not explain it. We argue that this scarcity is not an accident of attention, but the emergent consequence of four structural causes, each of which exerts a specific, mechanistically identifiable pressure against chronic-stage research.

First, the temporal asymmetry of signal dynamics. Responsive-hydrogel design is, at its core, trigger-driven, and its economic logic therefore follows the quality of the available triggers. Acute-stage cues—ROS and low pH—are high-amplitude, high-signal-to-noise, and sharply time-locked: a burst of ROS appears within hours and recedes, providing an unambiguous, reliably detectable gate (Section 3.1). Chronic-stage cues—CSPGs, N-cadherin, Pin1, and low-grade inflammation—are, by contrast, low-amplitude, sustained, and spatially diffuse, embedded in a noisy background of residual inflammation and ongoing remodeling. Their temporal windows are blurred rather than sharp, and their expression is highly heterogeneous across lesions. Because a trigger that is weak, noisy, and temporally ill-defined is a poor basis for a responsive element, the design paradigm is *systematically biased toward the acute phase*: it is simply easier—and more likely to yield a publishable, cleanly interpretable result—to build a hydrogel that answers a loud acute signal than one that must discriminate a faint chronic signal from background. This asymmetry is a sufficient cause, on its own, for the chronic phase's under-representation.

Second, the short observation windows of experimental models. The majority of *in vivo* SCI studies terminate at 4–8 weeks, yet glial-scar maturation and cystic-cavity consolidation typically require longer than 8 weeks to reach their mature, therapeutically relevant state (Section 3.3). The result is a *structural mismatch between observation duration and pathological maturation*: the chronic-phase biology that a scar-targeting hydrogel is meant to address is, in many studies, only beginning to develop when the experiment ends. Chronic-stage data are therefore not merely scarce but structurally incomplete—studies that might have revealed chronic-stage efficacy or failure are truncated before the relevant endpoint is reached. The observation window, not any lack of interest, is a binding constraint on chronic-stage evidence.

Third, the asymmetric cost of endpoint measurement. Acute-phase interventions are served by rapid, quantitative, and standardized readouts—motor scores, tissue-sparing histology, and molecular markers that are assayed within days to weeks and are well accepted by the field. Chronic-scar improvement, in contrast, lacks a comparably sensitive, standardized, and rapidly readable endpoint: scar thickness, CSPG density, and cyst volume are labor-intensive, low-throughput, and variably defined, and their relationship to functional recovery is indirect. This asymmetry *raises the cost of entry* for chronic-stage studies—more effort per unit of interpretable signal—which, under the same resource constraints, biases investigators toward the cheaper, faster acute-phase readouts. The chronic stage is not avoided because it is unimportant; it is avoided because it is expensive to measure.

Fourth, the engineering-feasibility bottleneck of multi-stage cascades. Embedding the chronic-scar node into a temporal chain is not a matter of adding one more payload; it requires *orthogonal trigger chemistry* (so that the scar-stage trigger does not cross-react with earlier ROS- or MMP-gated events), *multi-compartment payload architecture* (to sequester distinct cargoes and release them on independent schedules), and *degradation kinetics matched to the full repair timeline* (so that the scaffold persists through scar maturation without itself becoming a barrier). Each of these remains an unsolved material-science problem, and their conjunction—all three required simultaneously—represents a genuine, non-trivial engineering barrier. Chronic-stage responsiveness is therefore not simply under-explored; it is *harder to realize*, and this difficulty, rather than neglect, is a primary reason for its scarcity in the literature.

Taken together, these four causes compose a single thesis: the thinness of chronic-stage coverage is **not contingent but structural**—it is the predictable output of signal-dynamics asymmetry, truncated observation windows, costly endpoint measurement, and an unresolved engineering bottleneck acting in concert. This reframing matters for how the gap should be read. It is not a sign that the chronic scar is unimportant; on the contrary, it is precisely because the chronic scar sits at the intersection of the hardest triggers, the longest timescales, the costliest readouts, and the most demanding material requirements that it remains unsolved. Conquering the multi-step cascade—and thereby embedding the chronic-scar node into the temporal chain—is accordingly both a *difficult* and a *sharply defined* scientific problem: difficult because the four barriers are real and mutually reinforcing, and well-defined because each barrier points to a concrete, addressable research target rather than to a vague “more work is needed.”

Toward multi-step cascades. The logical endpoint of the time-programmable framework is a hydrogel that sequentially addresses three or more *distinct* pathological stages or mechanisms in the correct temporal order—for example, ROS scavenging → immunomodulation → scar inhibition → regeneration. The bibliometric synthesis (Section 2.4) shows that only a minority of the included studies currently employ ≥ 2 ordered events—i.e., satisfy the cascade criterion—and none yet spans three or more distinct pathological stages or mechanisms. The preceding mechanistic diagnosis identifies the precise levers that must be pulled to close this gap: for the signal-dynamics asymmetry, orthogonal trigger chemistries and threshold engineering that can discriminate a faint chronic cue from background; for the truncated observation window, longitudinal study designs that extend beyond scar maturation; for the costly endpoint problem, the development of standardized, high-throughput chronic-stage readouts; and for the engineering bottleneck, multi-compartment architectures whose degradation kinetics are matched to the full repair timeline. Each of these is a tractable, well-scoped target, and their pursuit defines the field's immediate research agenda. This is not merely an incremental goal; it is the transition from "responsive" to genuinely "programmed" materials.

The dosing dimension is missing from every temporal analysis. The systems surveyed, and this review with them, treat the hydrogel as though it were placed into a stationary lesion at time zero. In practice the timing of a staged release is set as much by the injection as by the chemistry. A scaffold implanted immediately after injury begins its program against a wound that is still haemorrhaging; the same scaffold placed at one week begins it against an established inflammatory infiltrate, and one placed at four weeks against a consolidated scar—three different starting points for the same release curve. Volume and concentration matter for the same reason: a larger bolus dilutes the payload over a larger tissue volume, lowering the local concentration that any threshold must detect, while a more concentrated gel risks a burst. The injury model compounds it further. Contusion leaves a graded spared rim, hemisection removes tissue and opens the cavity, and transection severs all tracts; the events a material is designed to match occur on different schedules in the three, so a program validated in a contusion is not automatically aligned in a transection. None of the 57 included studies reports how its release schedule shifts with injection timing, and none that compares two injury models.

Verifying the order, not just the release. Condition (c) requires that the timing of events be verified rather than asserted, yet none of the 57 included studies demonstrates the order of its own two events inside the cord. The half-times the index consumes are themselves in vitro quantities, read from buffer or enzyme release: in tissue, enzymatic degradation and mechanical clearance usually shorten them, so the score reports a lower bound on misalignment rather than a measurement made in the lesion. Four approaches could do so, and none is yet standard. Serial histology with spectrally distinct labels establishes co-location but resolves order only if the sampling is dense enough to catch the crossing. Intravital imaging through a chronic window resolves both space and time, at the cost of access restricted to the dorsal surface and observation restricted to hours to days. Microdialysis of the lesion interstitium recovers released cargo directly and yields a concentration-time curve, but its sampling interval and probe size confine it to small molecules. Activity-based or FRET reporters add real-time readout of a specific protease. A sequence claim resting on none of these describes the material, not the tissue.

Clinical translation and material safety. Translation imposes demands on biosafety, scalability, and regulatory pathways. A first concern is the **long-term biosafety of responsive payloads**: metal-based nanozymes (MnO_2, ZnO, nanoselenium) release ions whose chronic fate—bioaccumulation, off-target catalysis, secondary oxidative stress—has rarely been tracked beyond short rodent observation windows [8, 9, 150], and the host immune response to any implant (foreign-body reaction, fibrosis) is itself a determinant of outcome that a mature design literature now frames as deliberate immunomodulation rather than suppression [151]. Exogenous-stimulus platforms raise further questions about cumulative heating or field exposure to spared tissue [17, 20]. A second concern is **manufacturing reproducibility**: the graded crosslinks, layered compartments, and orthogonal triggers that confer temporal control also multiply the points at which scaling can perturb the release schedule. Third, **regulatory** frameworks for device–drug combination products are still maturing [152], and the cell-therapy experience—early trials establishing safety but not yet reproducible efficacy [153–155], highly variable preclinical efficacy across biomaterial combinations [156], and promising but early non-human-primate scaffold studies

[157]—underscores that standardization and integration, not biological activity, are the binding constraints. These issues are prerequisites, not polish, for engineering a hydrogel's timing to the human pathology.

Emerging modalities. Several nascent directions warrant attention: closed-loop systems coupling release with biosensing for feedback-regulated delivery [18]; the ferroptosis axis as a mechanistic target for ROS-scavenging nanozymes [9]; hybrid multi-modal coordination of exogenous-stimulus platforms with endogenous cascades [17, 20]; and enabling technologies—4D printing, integrated biosensors, and feedback-capable platforms [158, 159]. Cell-free routes, including hydrogel-encapsulated extracellular vesicles [160] and self-assembling peptide hydrogels [161], offer complementary strategies for paracrine and instructive regeneration. These directions collectively define the path from proof-of-concept toward clinical reality.

Beyond spinal cord injury. None of the three criteria is specific to the cord. Any indication whose pathology passes through distinguishable phases with different dominant signals poses the same design question, and the same two numbers — a window width W and a half-release time t½ — decide it: myocardial infarction (ischaemia, inflammation, fibrosis), stroke (hyperacute, acute, subacute, chronic), diabetic wound healing (haemostasis, inflammation, proliferation, remodelling), and bone defect repair are the obvious candidates, and each has a documented clinical clock. Spinal cord injury is used here because its phases are unusually well dated and because the interval to decompression is measured in hours, which makes the inversion visible rather than arguable; it is the clearest demonstration case, not the only one. The index transfers without modification — only W changes — and applying it to a second indication is the most direct test of whether the framework is a general design rule or a description of one field.

8. Conclusion

Spinal cord injury is a temporally staged disease, yet most hydrogel therapies to date are temporally static. We have argued that the therapeutic value of responsive hydrogels lies not in whether they respond, but in when and in what sequence they respond—the time-programmable principle. Framing the staged pathophysiology of SCI as the coordinate system for material design, we dissected the design principles (single-response versus cascade logic; response threshold, release kinetics, and degradation window) and mapped them across the four core mechanisms. Across this analysis, one conclusion recurs: efficacy tracks the temporal placement of an intervention, not its molecular identity—inflammation must be modulated early, ROS scavenged early and used as a gate, scar inhibition placed in the chronic middle, and regeneration delivered late. The first realizations of this staged logic (the ROS→MMP cascade and the dual-phase release-kinetics system) show the field is no longer merely aspirational, yet multi-step cascades spanning three or more pathological stages remain to be engineered.

The transition from single-point responsiveness to multi-stage temporal coordination is, in our view, the central trajectory of responsive-hydrogel research for SCI. The same inversion governs the choice of problems: the window that is easiest to design for is the hardest to reach, and the window that is easiest to reach is the one least designed for. Realizing it will require orthogonal triggers, multi-compartment architecture, tunable kinetics, and translation-oriented validation—but the payoff, if the framework holds, would be substantial: materials that no longer simply react to spinal cord injury, but are programmed to its timeline. The framework's first quantitative test puts the two best-designed systems at 0.6–0.8 on a scale where unity is perfect matching, and the remaining five between 0.06 and 0.44. Its value is not that it pronounces these systems failures, but that it makes the distance to unity visible, and therefore closable.

Scope of the framework. One tension should be stated plainly in closing. Time-programmability, as defined here, is a property of a design: a material either pre-encodes an ordered pair of events or it does not, and that can be read from its structure and its release data. Whether the encoded order is realised in tissue is a separate claim, and it is one that no study in this set has established. The framework is therefore useful in advance of that evidence-it tells a designer what to build and an experimenter what to measure-but “the next frontier” is a statement about design ambition, not a validated therapeutic strategy.

Declarations

CRediT authorship contribution statement

Jiongli Kuang: Conceptualization, Methodology, Investigation, Data curation, Formal analysis, Visualization, Writing – original draft. **Wenchun Wang:** Supervision, Project administration, Funding acquisition, Writing – review & editing.

Declaration of competing interest

The authors declare that they have no known competing financial interests or personal relationships that could have appeared to influence the work reported in this paper.

Funding

This work was supported by the General Hospital of Western Theater Command medical project (grant number 2024-YGJC-B01), the Science and Technology Research Project of the Sichuan Provincial Administration of Traditional Chinese Medicine (grant number 25MSZX493; “Mechanism by which valtrate promotes axonal regeneration after spinal cord injury via the Nrf2/HO-1 pathway”), and the Chengdu Health Commission medical project (grant number 2024032). The funders had no role in the design of the review, in the selection or coding of the studies, or in the decision to submit the manuscript.

Data availability

All data supporting this review are contained within the article and its supplementary files (Supplementary Tables S1–S4, Supplementary Figs. S1–S2). The coded dataset of the 57 included studies is Supplementary Table S1; the window assignment for each payload is Supplementary Table S2; the sensitivity analysis is Supplementary Table S3; and the digitised release values underlying Figs. 5 and 7 and Table 2 are Supplementary Table S4. The coding table, the window assignments, the sensitivity analysis and the digitised curves are also archived at Zenodo under DOI 10.5281/zenodo.23858212 (Kuang and Wang, 2026), together with a short script, tmi.py, that recomputes the temporal matching index from the digitised curves and reproduces the fourteen payload scores of Table 2. No new primary data were generated.

Acknowledgements

The authors thank colleagues in the Department of Rehabilitation Medicine for discussion of the clinical timing data. No writing assistance was used beyond the language editing declared below.

Declaration of generative AI in scientific writing

During the preparation of this work the authors used a large language model to improve the readability and English expression of the manuscript. After using this tool, the authors reviewed and edited the content as needed and take full responsibility for the content of the publication. The tool was not used to generate scientific claims, to select or interpret the cited literature, or to produce any of the quantitative results reported here.

References

1. Ahuja CS, Wilson JR, Nori S, Kotter MRN, Druschel C, Curt A et al (2017) Traumatic spinal cord injury. Nat Rev Dis Primers 3:17018
2. Alizadeh A, Dyck SM, Karimi-Abdolrezaee S (2019) Traumatic spinal cord injury: an overview of pathophysiology, models and acute injury mechanisms. Front Neurol 10:282
3. Omidian H, Chowdhury SD, Cubeddu LX (2024) Hydrogels for neural regeneration: exploring new horizons. Materials 17:3472

4. Ahuja CS, Nori S, Tetreault L, Wilson J, Kwon B, Harrop J et al (2017) Traumatic spinal cord injury—repair and regeneration. Neurosurgery 80:S9–S22
5. Rotaru-Zavaleanu AD, Bica M, Dinescu S-N, Ruscu MA, Vasile RC, Zavate AC et al (2025) Bioactive hydrogels for spinal cord injury repair: emphasis on gelatin and its derivatives. Gels 11:497
6. Han C, Jiao J, Gong C, Li J, Zhao M, Lu X (2025) Multidimensional exploration of hydrogels as biological scaffolds for spinal cord regeneration: mechanisms and future perspectives. Front Bioeng Biotechnol 13:1576524
7. Moghaddasi M, Oktay B, Bingol AB, Yanikoglu R, Muslu M, Ozbolat IT et al (2025) Conductive nanocomposite hydrogels for neural tissue engineering: a systematic scoping review of recent trends. Adv Sci 12:e2416085
8. Yuan Y, Xu M, Feng L, Zhong W, Zhang L, Du R et al (2024) Nanozyme hydrogels promote nerve regeneration in spinal cord injury by reducing oxidative stress. ACS Appl Mater Interfaces 16:59949–59961
9. Ding J, Gao B, Sang Z, Dai Z, Chen Z, Mei X (2025) Promoting spinal cord injury repair by using ZnO@MOFs nanozymes functionalized hydrogel through the ROS microenvironment regulating pathway. Regen Biomater 12:rbaf095
10. Cao J, Zhang X, Guo J, Wu J, Lin L, Lin X et al (2025) An engineering-reinforced extracellular vesicle–integrated hydrogel with an ROS-responsive release pattern mitigates spinal cord injury. Sci Adv 11:eads3398
11. Shen H, Xu B, Yang C, Xue W, You Z, Wu X et al (2022) A DAMP-scavenging, IL-10-releasing hydrogel promotes neural regeneration and motor function recovery after spinal cord injury. Biomaterials 280:121279
12. Lumelsky N (2021) Creating a pro-regenerative tissue microenvironment: local control is the key. Front Bioeng Biotechnol 9:714572
13. Liu Z, Yu C, Li Z, Wang X, Shang D, Dong W (2025) Matrix metalloproteinase-triggered self-assembling peptides for biomedical applications. J Mater Chem B 13:8298–8334
14. Liu Q, Peng S, Tang Q, Li C, Chen J, Pang P et al (2024) A N-cadherin nano-antagonist hydrogel enhances recovery from spinal cord injury by impeding glial scarring. Adv Funct Mater 34:2404563
15. Zhu S, Wu Q, Ying Y, Mao Y, Lu W, Xu J et al (2024) Tissue-adaptive BSA hydrogel with dual release of PTX and bFGF promotes spinal cord injury repair via glial scar inhibition and axon regeneration. Small 20:2401407
16. Zhang R, Tang T, Zhuang H, Wang P, Yu H, Xu H et al (2024) Temperature-sensitive sodium β-glycerophosphate/chitosan hydrogel loaded with all-trans retinoic acid regulates Pin1 to inhibit the formation of spinal cord injury-induced rat glial scar. Bioeng Transl Med 10:e10729
17. Yang CY, Meng Z, He Z, Ma P, Hou Z, Kim K et al (2024) Engineering neuroregenerative microenvironment via aligned hydrogel-assisted magnetic stimulation for complete spinal cord injury repair. Eng Regen 5:139–152
18. Fan Z, Zhang G, Zhan W, Wang J, Wang C, Yue Q et al (2025) Hyaluronidase-responsive hydrogel loaded with magnetic nanoparticles combined with external magnetic stimulation for spinal cord injury repair. Mater Today Bio 30:101378
19. Ahuja CS, Badhiwala JH, Fehlings MG (2020) Time is spine: the importance of early intervention for traumatic spinal cord injury. Spinal Cord 58:1037–1039
20. Liu W, Liu Q, Li Z, Zhang C, Li Z, Ke H et al (2025) Multifunctional magneto-electric and exosome-loaded hydrogel enhances neuronal differentiation and immunoregulation through remote non-invasive electrical stimulation for neurological recovery after spinal cord injury. Bioact Mater 48:510–528
21. Chen H, Wang W, Yang Y, Zhang B, Li Z, Chen L et al (2025) A sequential stimuli-responsive hydrogel promotes structural and functional recovery of severe spinal cord injury. Biomaterials 316:122995
22. Zhang R, Zhang M, Chen L, Jiang L, Zou C, Li N et al (2024) Dual-phase SilMA hydrogel: a dynamic scaffold for sequential drug release and enhanced spinal cord repair via neural differentiation and immunomodulation. Front Bioeng Biotechnol 12:1501488
23. Zhong Z, Zhao K, Hu H, Chen X, Zheng W, Gao C (2026) Self-adaptive hydrogels for treatment of spinal cord injury. J Control Release 394:114854

24. Qian D, Xu J, Zhang X, Hu F, Cao S, Dong Y et al (2024) Microenvironment self-adaptive nanomedicine promotes spinal cord repair by suppressing inflammation cascade and neural apoptosis. Adv Mater 36:e2307624
25. Luo Y, Jiang P, Huang D, Li H, He J, Shen R et al (2026) Synergistic mitochondrial homeostasis regulation and cholinergic circuits reconstruction via a one-step synthesized multifunctional hydrogel facilitates spinal cord injury repair. Bioact Mater 59:370–395
26. Wu C, Chen X, Zhao X, Chen Y, Zhou H, Deng Y et al (2024) Screening strategy identified idebenone loaded ROS-responsive nano-polyphenolic vesicle for spinal cord injury therapy. Mater Des 242:112972
27. Zhao J, Xiong Y, Wang X, Wang Y, He J, Wu F (2025) Succinic acid-based biodegradable hydrogels drive Bv2 microglial polarization by ATP metabolism, Compos. Part B Eng 298:112383
28. Paone LS, Jin Y, Bouyer J, Fischer I, Galie PA (2026) Development of a multifunctional, injectable biomaterial using hyaluronan as a bioactive nanocarrier. Biomaterials 324:123505
29. Cai M, Chen L, Wang T, Liang Y, Zhao J, Zhang X et al (2023) Hydrogel scaffolds in the treatment of spinal cord injury: a review. Front Neurosci 17:1211066
30. Xu L, Zhou S, Dai X, Gu X, Ouyang Z (2025) Tissue engineering and spinal cord injury repair. Engineering 46:60–72
31. Luo J, Ding Y, Niu J, Li M, Wang Y, Liu D et al (2026) A dual-responsive bilayer hydrogel orchestrates immunomodulation and axonal regeneration after spinal cord injury. Mater Des 267:116364
32. Liu Y, Xia M, Zhang C, Zhang Y, Li Z, Wang W et al (2026) Sequential delivery of STING inhibitor and rapamycin by a Sr-Zn mesoporous bioactive glass platform for spinal cord injury repair. J Control Release 398:115198
33. Lima R, Monteiro A, Salgado AJ, Monteiro S, Silva NA (2022) Pathophysiology and therapeutic approaches for spinal cord injury. Int J Mol Sci 23:13833
34. Anjum A, Yazid MD, Daud MF, Idris J, Ng AMH, Naicker AS et al (2020) Spinal cord injury: pathophysiology, multimolecular interactions, and underlying recovery mechanisms. Int J Mol Sci 21:7533
35. McDonald JW, Sadowsky C (2002) Spinal cord injury. Lancet 360:1884
36. Bartanusz V, Jezova D, Alajajian B, Digicaylioglu M (2011) The blood–spinal cord barrier: Morphology and clinical implications. Ann Neurol 70:194–206
37. Jin L-Y, Li J, Wang K-F, Xia W-W, Zhu Z-Q, Wang C-R et al (2021) Blood–spinal cord barrier in spinal cord injury: a review. J Neurotrauma 38:1203–1224
38. Park E, Velumian AA, Fehlings MG (2004) The role of excitotoxicity in secondary mechanisms of spinal cord injury: a review with an emphasis on the implications for white matter degeneration. J Neurotrauma 21:754–774
39. Hou J, Klippel K, Bose P (2025) Glutamate excitotoxicity: a key secondary injury mechanism of traumatic brain injury and spinal cord injury. Front Biosci 30:38904
40. Schmidt J, Quintá HR (2023) Mitochondrial dysfunction as a target in spinal cord injury: intimate correlation between pathological processes and therapeutic approaches, Neural Regen. Res 18:2161–2166
41. Mehta A, Prabhakar M, Kumar P, Deshmukh R, Sharma P (2013) Excitotoxicity: Bridge to various triggers in neurodegenerative disorders. Eur J Pharmacol 698:6–18
42. David S, Kroner A (2011) Repertoire of microglial and macrophage responses after spinal cord injury. Nat Rev Neurosci 12:388–399
43. Li Q, Barres BA (2017) Microglia and macrophages in brain homeostasis and disease. Nat Rev Immunol 18:225–242
44. Yang Q, Zhou J (2018) Neuroinflammation in the central nervous system: Symphony of glial cells. Glia 67:1017–1035
45. Tang H, Gu Y, Jiang L, Zheng G, Pan Z, Jiang X (2023) The role of immune cells and associated immunological factors in the immune response to spinal cord injury. Front Immunol 13:1070540
46. Kigerl KA, Gensel JC, Ankeny DP, Alexander JK, Donnelly DJ, Popovich PG (2009) Identification of two distinct macrophage subsets with divergent effects causing either neurotoxicity or regeneration in the injured mouse spinal cord. J Neurosci 29:13435–13444

47. Ransohoff RM (2016) A polarizing question: do M1 and M2 microglia exist? Nat Neurosci 19:987–991
48. Sofroniew MV, Vinters HV (2010) Astrocytes: biology and pathology. Acta Neuropathol 119:7–35
49. Luo J, Hu W, Gao X, Bai J, Sheng L, Yang H et al (2024) Macrophage polarization-based biomaterials for repairing spinal cord injury. ACS Mater Lett 6:5438–5453
50. Milich LM, Choi JS, Ryan C, Cerqueira SR, Benavides S, Yahn SL et al (2021) Single-cell analysis of the cellular heterogeneity and interactions in the injured mouse spinal cord. J Exp Med 218:e20210040
51. Hakim R, Zachariadis V, Sankavaram SR, Han J, Harris RA, Brundin L et al (2021) Spinal cord injury induces permanent reprogramming of microglia into a disease-associated state which contributes to functional recovery. J Neurosci 41:8441–8459
52. Sofroniew MV (2009) Molecular dissection of reactive astrogliosis and glial scar formation. Trends Neurosci 32:638–647
53. Liddelow SA, Guttenplan KA, Clarke LE, Bennett FC, Bohlen CJ, Schirmer L et al (2017) Neurotoxic reactive astrocytes are induced by activated microglia. Nature 541:481–487
54. Fan Y-Y, Huo J (2021) A1/A2 astrocytes in central nervous system injuries and diseases: angels or devils? Neurochem Int 148:105080
55. Bradbury EJ, Moon LDF, Popat RJ, King VR, Bennett GS, Patel PN et al (2002) Chondroitinase ABC promotes functional recovery after spinal cord injury. Nature 416:636–640
56. Silver J, Miller JH (2004) Regeneration beyond the glial scar. Nat Rev Neurosci 5:146–156
57. Sharma K, Selzer ME, Li S (2012) Scar-mediated inhibition and CSPG receptors in the CNS. Exp Neurol 237:370–378
58. Shen Y, Tenney AP, Busch SA, Horn KP, Cuascut FX, Liu K et al (2009) PTPσ Is a Receptor for Chondroitin Sulfate Proteoglycan, an Inhibitor of Neural Regeneration. Science 326:592–596
59. Faulkner JR, Herrmann JE, Woo MJ, Tansey KE, Doan NB, Sofroniew MV (2004) Reactive astrocytes protect tissue and preserve function after spinal cord injury. J Neurosci 24:2143–2155
60. Anderson MA, Burda JE, Ren Y, Ao Y, O'Shea TM, Kawaguchi R et al (2016) Astrocyte scar formation aids central nervous system axon regeneration. Nature 532:195–200
61. Escartin C, Galea E, Lakatos A, O'Callaghan JP, Petzold GC, Serrano-Pozo A et al (2021) Reactive astrocyte nomenclature, definitions, and future directions. Nat Neurosci 24:312–325
62. Anderson MA, O'Shea TM, Burda JE, Ao Y, Barlatey SL, Bernstein AM et al (2018) Required growth facilitators propel axon regeneration across complete spinal cord injury. Nature 561:396–400
63. Shan B, Wu F (2023) Hydrogel-Based Growth Factor Delivery Platforms: Strategies and Recent Advances. Adv Mater 36:2210707
64. Ma D, Wu X, Ma Y, Tan H, Yin H, Zhou Z et al (2026) Advances in Microenvironment-Responsive Biomaterials for Spinal Cord Injury Repair. Adv Healthc Mater 15:e05952
65. Li Z, Yu H, Wang Z, Duan H, Li M, Liao J et al (2025) Recent advances in nanotechnology for repairing spinal cord injuries. Biomaterials 323:123422
66. Guo D, Xiao L, Xu K, Li H, Li Z, Pan Y et al (2026) Harnessing conductive hydrogels for spinal cord injury repair: From bioelectrical design to neural circuit reconstruction. Mater Today Adv 31:100934
67. Ghosh S, Ghosh S, Sharma H, Bhaskar R, Han SS, Sinha JK (2024) Harnessing the power of biological macromolecules in hydrogels for controlled drug release in the central nervous system: A review. Int J Biol Macromol 254:127708
68. Mozhdehbakhsh Mofrad Y, Asiaei S, Shaygani H, Cheraghi F, Amirsaadat S, Soltani M et al (2025) Advances in smart hydrogels for nerve repair: A review focusing on criteria and applications. J Sci Adv Mater Devices 10:100996
69. Li N, He J (2024) Hydrogel-based therapeutic strategies for spinal cord injury repair: Recent advances and future prospects. Int J Biol Macromol 277:134591

70. Sun J, Cao Y, Liu P, Gao J (2025) Multifunctional hydrogels loaded with drugs for spinal cord injury repair. RSC Adv 15:32553–32559
71. Mukherjee N, Adak A, Ghosh S (2020) Recent trends in the development of peptide and protein-based hydrogel therapeutics for the healing of CNS injury. Soft Matter 16:10046–10064
72. Jin S, Ma Y, Zhang S (2026) Current status and future prospects of functionalized mesenchymal stem cells for the treatment of spinal cord injury. J Orthop Transl 58:101125
73. Li Q, Shao X, Dai X, Guo Q, Yuan B, Liu Y et al (2022) Recent trends in the development of hydrogel therapeutics for the treatment of central nervous system disorders. NPG Asia Mater 14:14
74. Gao H, Shen H, Zhang X, Liu Y, Shang Y, Sun S et al (2025) Revolutionizing neural regeneration with smart responsive materials: Current insights and future prospects. Bioact Mater 52:393–421
75. Zhang D, Li Z, Yang L, Ma H, Chen H, Zeng X (2023) Architecturally designed sequential-release hydrogels. Biomaterials 303:122388
76. Lin X, Dong Y, Chew SY (2021) Injectable hydrogels in stroke and spinal cord injury treatment: a review on hydrogel materials, cell–matrix interactions and glial involvement. Mater Adv 2:2561–2583
77. Feng L, Zhu S, Zhang R, Xu T, Wang H, Zheng N et al (2025) Injectable natural polymer-based hydrogels: a promising minimally invasive therapy for future neural tissue repair. Chem Eng J 525:170637
78. Kaplan B, Levenberg S (2022) The role of biomaterials in peripheral nerve and spinal cord injury: a review. Int J Mol Sci 23:1244
79. Badeau BA, Comerford MP, Arakawa CK, Shadish JA, DeForest CA (2018) Engineered modular biomaterial logic gates for environmentally triggered therapeutic delivery. Nat Chem 10:251–258
80. Gawade PM, Shadish JA, Badeau BA, DeForest CA (2019) Logic-based delivery of site-specifically modified proteins from environmentally responsive hydrogel biomaterials. Adv Mater 31:1902462
81. Webber MJ, Appel EA, Meijer EW, Langer R (2016) Supramolecular biomaterials. Nat Mater 15:13–26
82. Han Y, Cao Y, Lei H (2022) Dynamic covalent hydrogels: strong yet dynamic. Gels 8:577
83. Badeau BA, DeForest CA (2019) Programming stimuli-responsive behavior into biomaterials. Annu Rev Biomed Eng 21:241–265
84. Yilmaz AS, Pepe A, Latifi N, Sawyer GW, Dunne MR (2026) Stimuli-responsive hydrogels in targeted cancer therapy: a systematic review of materials, mechanisms, and delivery strategies. Mater Des 261:115318
85. Luo Y, Li J, Li B, Xia Y, Wang H, Fu C (2021) Physical cues of matrices reeducate nerve cells, Front. Cell Dev Biol 9:731170
86. Zhang R, Zou C, Jiang L, Bai B, Li C, Zhang C et al (2025) Repair of spinal cord injury using a time-specific four-dimensional multifunctional hydrogel with anti-inflammatory and neuronal differentiated microenvironments. Biomater Sci 13:4153–4167
87. Li Y, Liang Y, He C, Yao R, Jian K, Shi L (2025) A dual-drug sequential delivery hydrogel for programmatic microglia/macrophage polarization and function recovery in spinal cord injury. Mater Today Bio 35:102365
88. Zhou HY, Wang X, Li Y, Wang D, Zhou XZ, Xiao N et al (2025) Dynamic development of microglia and macrophages after spinal cord injury. Neural Regen Res 20:3606–3619
89. Wang J, Tian F, Cao L, Du R, Tong J, Ding X et al (2023) Macrophage polarization in spinal cord injury repair and the possible role of microRNAs: A review. Heliyon 9:e22914
90. Fu SP, Chen SY, Pang QM, Zhang M, Wu XC, Wan X et al (2022) Advances in the research of the role of macrophage/microglia polarization-mediated inflammatory response in spinal cord injury. Front Immunol 13:1014013
91. Walsh CM, Wychowaniec JK, Brougham DF, Dooley D (2022) Functional hydrogels as therapeutic tools for spinal cord injury: new perspectives on immunopharmacological interventions. Pharmacol Ther 234:108043

92. Hou Y, Jiang Y, Niu X, Li Y, Zhu T, Rong H et al (2026) Curcumin-loaded multifunctional hydrogel drives spinal cord neural regeneration through immune microenvironment remodeling. Nano Res 19:94908574
93. Zhou J, Fang C, Rong C, Luo T, Liu J, Zhang K (2023) Reactive oxygen species-sensitive materials: a promising strategy for regulating inflammation and favoring tissue regeneration. Smart Mater Med 4:427–446
94. Stockwell BR, Friedmann Angeli JP, Bayir H, Bush AI, Conrad M, Dixon SJ et al (2017) Ferroptosis: A regulated cell death nexus linking metabolism, redox biology, and disease. Cell 171:273–285
95. Bai X-Y, Liu X-L, Deng Z-Z, Wei D-M, Zhang D, Xi H-L et al (2023) Ferroptosis is a new therapeutic target for spinal cord injury. Front Neurosci 17:1136143
96. Liu Y, Wang Y, Wang X, Zeng W, Zhang Z, Zhang Z et al (2025) Synergistic Antioxidant and Anti-Ferroptosis Therapy via BPNS-Encapsulated Thermoresponsive Chitosan Hydrogel for Spinal Cord Injury Regeneration. Pharmaceutics 17:573
97. Sun Y, Zhang J, Gu Y, Liu T, Chen L (2024) Biomineralized MnO_2 Nanoparticle-Constituted Hydrogels Promote Spinal Cord Injury Repair by Modulating Redox Microenvironment and Inhibiting Ferroptosis. Pharmaceutics 16:1057
98. Li L, Cao Y, Zhang X, Guo J, Lin Z, Zhou P et al (2025) Injectable ROS homeostasis protective hydrogel inhibiting microglial ferroptosis through the Nrf2/Slc7a11/Gpx4 to alleviate neuropathic pain and promote spinal cord injury repair. Redox Biol 86:103816
99. Su H, Li K, Li H, Huang T, Jin S, Su Z et al (2026) Nanozyme-integrated metal polyphenol coordination hydrogels for microenvironment remodeling and spinal cord injury repair. Chem Eng J 547:181082
100. Zhao L, Zhang C, Li J, Guo Y, Meng J, Yin Y et al (2026) Dynamic ROS-responsive injectable hydrogel incorporating nanozymes for spinal cord repair by alleviating oxidative stress and neuronal ferroptosis. Biomaterials 330:124059
101. Liu D, Lu G, Shi B, Ni H, Wang J, Qiu Y et al (2023) ROS-Scavenging Hydrogels Synergize with Neural Stem Cells to Enhance Spinal Cord Injury Repair via Regulating Microenvironment and Facilitating Nerve Regeneration. Adv Healthc Mater 12:2300123
102. Li Z, Zhao Q, Zhou J, Li Y, Zheng Y, Chen L (2025) A reactive oxygen species-responsive hydrogel loaded with Apelin-13 promotes the repair of spinal cord injury by regulating macrophage M1/M2 polarization and neuroinflammation. J Nanobiotechnol 23:12
103. Cao J, Wu J, Mu J, Lin L, Zhang X, Huang T et al (2023) ROS filter coating scaffold protects 3D mesenchymal stem cell spheroids for dual-phase treatment of spinal cord injury. Chem Eng J 462:142192
104. Ren L, Zhou X, Feng L, Sun G (2026) ROS-scavenging and oxygen-generating MgMn-LDH integrated smart injectable hydrogel for microenvironment-reprogrammable spinal cord injury repair. Mater Adv 7:3586–3607
105. Zhu X, Liu Z, Li K, Fan Y, Yang K, Sun X et al (2026) GDNF-enriched small extracellular vesicle-loaded ROS-scavenging hydrogel promotes neural regeneration after spinal cord injury. Adv Healthc Mater e71806
106. Gong L, Gu Y, Han X, Luan C, Liu C, Wang X et al (2022) Spatiotemporal Dynamics of the Molecular Expression Pattern and Intercellular Interactions in the Glial Scar Response to Spinal Cord Injury. Neurosci Bull 39:213–244
107. Hou Z, Shang S, Sun H, He Y, Guo S, Sun M et al (2026) Targeting the glial-fibrotic scar microenvironment after spinal cord injury: From integrated protection to systematic regulation of regenerative balance. J Orthop Transl 58:101120
108. Bradbury EJ, Burnside ER (2019) Moving beyond the glial scar for spinal cord repair. Nat Commun 10:3879
109. Xiao L, Shi K, Li W, Liu J, Xie P, Hu Z et al (2025) Targeting Fibrotic Scarring by Mechanoregulation of Il11ra1+/Itga11 + Fibroblast Patterning Promotes Axon Growth after Spinal Cord Injury. Adv Sci 12:e13476
110. Wang Q, Zhang H, Xu H, Zhao Y, Li Z, Li J et al (2018) Novel multi-drug delivery hydrogel using scar-homing liposomes improves spinal cord injury repair. Theranostics 8:4429–4446
111. Wu T, Li Y, Wu Z, Wang Z, Li Y, Jian K et al (2024) Enzyme-immobilized nanoclay hydrogel simultaneously reduces inflammation and scar deposition to treat spinal cord injury. Chem Eng J 484:149642
112. Zheng Y, Zhang Z, Fu Z, Wang Q, Zhang S, Zhang T et al (2025) Disrupting CSPG-driven microglia-astrocyte crosstalk enables scar-free repair in spinal cord injury. Adv Sci 13:e16269

113. Cunha RS, Rossi EA, Santana TAS, Costa-Ferro ZSM, Souza BSF (2025) Chondroitinase ABC in spinal cord injury: advances in delivery strategies and therapeutic synergies. Front Bioeng Biotechnol 13:1604502
114. Zhou T, Lin Y, Wang Y, Lin L, Li J, Tang N et al (2026) Impeding glial scarring hyperplasia and activating axon neogenesis via immunomodulatory microneedle patch for spinal cord repair. J Nanobiotechnol 24:653
115. Li Y, Wang Z, Pei S, Chen R, Li Y, Liang Y et al (2024) Bisphosphonate-Based Hydrogel with pH-Responsive Minocycline Release Inhibits Microglia/Macrophages of M1 Polarization for Spinal Cord Injury Therapy. ACS Mater Lett 6:553–565
116. Wang Y, Liu J, Li P, Peng Z, Zhang Y, Liu Y et al (2025) Nasal Delivery of Engineered Exosomes via a Thermo-Sensitive Hydrogel Depot Reprograms Glial Cells for Spinal Cord Repair. Adv Sci 12:e04486
117. Duncan GJ, Manesh SB, Hilton BJ, Assinck P, Plemel JR, Tetzlaff W (2020) The fate and function of oligodendrocyte progenitor cells after traumatic spinal cord injury. Glia 68:227–245
118. Pukos N, Goodus MT, Sahinkaya FR, McTigue DM (2019) Myelin status and oligodendrocyte lineage cells over time after spinal cord injury: what do we know and what still needs to be unwrapped? Glia 67:2178–2202
119. Bonosi L, Silven MP, Biancardino AA, Sciortino A, Giammalva GR, Scerrati A et al (2022) Stem cell strategies in promoting neuronal regeneration after spinal cord injury: a systematic review. Int J Mol Sci 23:12996
120. Pinelli F, Pizzetti F, Veneruso V, Petillo E, Raghunath M, Perale G et al (2022) Biomaterial-mediated factor delivery for spinal cord injury treatment. Biomedicines 10:1673
121. Li W, Zhang W, Zheng H, Zhang Y, Feng Y, Xie Y et al (2026) A dual-functional engineered exosome-laden hydrogel redirects endogenous neural stem cell fate for spinal cord injury repair. Bioact Mater 62:899–919
122. Du H, Yang X, Qi Z, Zhao J, Zhang R, Wang J et al (2025) Conductive hydrogel combined with electrical stimulation remodels the microenvironment for nerve regeneration to promote spinal cord injury repair. J Nanobiotechnol 24:76
123. Zhang Q, Wei F, Zhang L, Liang C, Zhuang Y, Jiang N et al (2025) Electroacupuncture at Huatuo-Jiaji acupoints combined with conductive hydrogel synergistically improves bladder and motor functions after spinal cord injury. Mater Today Bio 35:102335
124. Liu M, Zhang W, Han S, Zhang D, Zhou X, Guo X et al (2024) Multifunctional Conductive and Electrogenic Hydrogel Repaired Spinal Cord Injury via Immunoregulation and Enhancement of Neuronal Differentiation. Adv Mater 36:2313672
125. Liu Q, Wang W, Yang H, Wang Y, Shi Y, Chen Y et al (2024) Microenvironment-Responsive Injectable Conductive Hydrogel for Spinal Cord Injury Repair. Adv Funct Mater 34:2406376
126. Wu P, Chen P, Xu C, Mu C, Zou X, Yang K et al (2024) Biodegradable conductive hydrogels generating magnetic-field-driven wireless electrical stimulation enhance the spinal cord injury repair. Nano Energy 130:110123
127. Sang Z, Liang Z, Xuelian Huang G, Chen Z, Ren X, Mei X (2024) NIR sensitive ZnO QDs decorated MXene hydrogel promotes spinal cord repair via tunable controlled release of Zn2 + and regulating ROS microenvironment of mitochondrion. Chem Eng J 489:151343
128. Yang CY, Meng Z, Yang K, He Z, Hou Z, Yang J et al (2023) External magnetic field non-invasively stimulates spinal cord regeneration in rat via a magnetic-responsive aligned fibrin hydrogel. Biofabrication 15:035022
129. Xu L, Mu J, Ma Z, Lin P, Xia F, Hu X et al (2023) Nanozyme-Integrated Thermoresponsive In Situ Forming Hydrogel Enhances Mesenchymal Stem Cell Viability and Paracrine Effect for Efficient Spinal Cord Repair. ACS Appl Mater Interfaces 15:37193–37204
130. Liu D, Zhu Y, Li C, Jian X, Chang S, Mao S et al (2025) Mitochondrion-Targeting Piezoelectric Nanocomposite Hydrogels for Spinal Cord Injury Repair via Directing Neuronal Differentiation of Neural Stem Cells. Adv Funct Mater 36:e17907
131. Yuan W, Zhao P, Shen W, Zhang Y, Dai W, Zhong H et al (2026) A printable blue-light photocurable gelatin methacryloyl/silk fibroin hydrogel loaded with salvianolic acid B for enhanced spinal cord repair. Int J Biol Macromol 376:153399
132. Chiang MY, Cheng HW, Lo YC, Wang WC, Chang SJ, Cheng CH et al (2021) 4D spatiotemporal modulation of biomolecules distribution in anisotropic corrugated microwrinkles via electrically manipulated microcapsules within

hierarchical hydrogel for spinal cord regeneration. Biomaterials 271:120762

133. Yu C, Yao F, Li J (2022) Rational design of injectable conducting polymer-based hydrogels for tissue engineering. Acta Biomater 139:4–21
134. Sun Y, Sun M, Lin X, Sun Y, Mei D, Zhang H et al (2026) MMP-responsive hydrogel: a new approach for tissue repair and regeneration. Mater Des 263:115573
135. Shi J, Yu L, Ding J (2021) PEG-based thermosensitive and biodegradable hydrogels. Acta Biomater 128:42–59
136. Shahemi NH, Mahat MM, Asri NAN, Amir MA, Ab Rahim S, Kasri MA (2023) Application of conductive hydrogels on spinal cord injury repair: a review, ACS Biomater. Sci Eng 9:4045–4085
137. Sun Z, Zhu D, Zhao H, Liu J, He P, Luan X et al (2023) Recent advance in bioactive hydrogels for repairing spinal cord injury: material design, biofunctional regulation, and applications. J Nanobiotechnol 21:238
138. Zhang W, Hu Q, Li W, Zhou X, Liu M, Lu J et al (2026) Spatiotemporal liposome-zwitterionic nano-hydrogel orchestrates immunomodulation-neurogenesis in spinal cord injury repair. Mater Today Bio 38:103100
139. Zhao J, Zhong H, Hu B, Wang H, Liu S, Li B et al (2026) Sequential dual-drug delivery biomimetic hydrogel for temporal orchestration of acute neuroprotection and chronic regeneration in spinal cord injury. Acta Biomater 213:214–232
140. Wei Z, Huang S, Zhang W, Wen J, Zhou X, He W et al (2025) Nanogel Integrated Zwitterionic Injectable Hydrogel with Sequential Drug-Releasing Capability for the Programmable Repair of Spinal Cord Injury. Adv Sci 13:e10976
141. Sha Q, Li Y, Wu Z, Wang Y, Fang Y, Liu A et al (2026) Injectable adhesive hydrogel with self-assembled dual-enzyme nanofibers for spatiotemporal modulation of inflammation and axon regeneration after spinal cord injury. Chem Eng J 542:178257
142. Ai Y, Hu C, Wang Y, Liu Y, Liu R, Xu H et al (2025) Core-shell hydrogel microspheres with sequential delivery of cerium oxide nanoparticles and spinal white matter extracellular matrix for improved functional recovery in spinal cord injury. Chem Eng J 508:160861
143. Wang H, Sun Y, Wang S, Wang W, Tang J, Li Z et al (2026) Spatiotemporal Co-Delivery of Hydrogen and Magnesium via Microneedle Patches for Neuroinflammation Modulation After Spinal Cord Injury: A Multi-Modal In Vivo Study. Small 22:e14854
144. Li Y, Hu J, Ran B, Zhong H, Zhong N, Zhong Y et al (2026) Dual-responsive PDA-HP hydrogel enables mitochondria-targeted mild photothermal therapy for spinal cord repair. Mater Today Bio 37:102783
145. Tang Y, Xu Z, Tang J, Xu Y, Li Z, Wang W et al (2023) Architecture-Engineered Electrospinning Cascade Regulates Spinal Microenvironment to Promote Nerve Regeneration. Adv Healthc Mater 12:2202658
146. Bao X, Sun J, Gao X, Xu M, Dong C, Pan H (2026) A spatiotemporally controlled MNE@PDA-Diz/GP hydrogel system: enhancing spinal cord injury repair via ROS scavenging, calcium influx inhibition, and macrophage polarization. RSC Adv 16:12458–12474
147. Aarhus M, Mirzamohammadi J, Rønning PA, Strøm M, Glott T, Rizvi SAM et al (2024) Time from injury to acute surgery for patients with traumatic cervical spinal cord injury in South-East Norway. Front Neurol 15:1420530
148. Tuli S, Tuli J, Coleman WP, Geisler FH, Krassioukov A (2007) Hemodynamic parameters and timing of surgical decompression in acute cervical spinal cord injury. J Spinal Cord Med 30:482–490
149. Zhao Y, Tang F, Xiao Z, Han G, Wang N, Yin N et al (2017) Clinical study of NeuroRegen scaffold combined with human mesenchymal stem cells for the repair of chronic complete spinal cord injury. Cell Transpl 26:891–900
150. Sisakhtnezhad S, Rahimi M, Mohammadi S (2023) Biomedical applications of MnO_2 nanomaterials as nanozyme-based theranostics. Biomed Pharmacother 163:114833
151. Whitaker R, Hernaez-Estrada B, Hernandez RM, Santos-Vizcaino E, Spiller KL (2021) Immunomodulatory biomaterials for tissue repair. Chem Rev 121:11305–11335
152. Trubelja A, Kasper FK, Farach-Carson MC, Harrington DA (2022) Bringing hydrogel-based craniofacial therapies to the clinic. Acta Biomater 138:1–20

153. Abraham ME, Song F, Glasser A, Lieberman G, Martin JR, Ciacci JD (2026) Intraparenchymal stem cell transplantation for spinal cord injury: a review of clinical trials. Regen Med 21:55–66
154. Shinozaki M, Nagoshi N, Nakamura M, Okano H (2021) Mechanisms of stem cell therapy in spinal cord injuries. Cells 10:2676
155. Zipser CM, Cragg JJ, Guest JD, Fehlings MG, Jutzeler CR, Anderson AJ et al (2022) Cell-based and stem-cell-based treatments for spinal cord injury: evidence from clinical trials. Lancet Neurol 21:659–670
156. Guijarro-Belmar A, Varone A, Baltzer MR, Kataria S, Tanriver-Ayder E, Watzlawick R et al (2022) Effectiveness of biomaterial-based combination strategies for spinal cord repair—a systematic review and meta-analysis of preclinical literature. Spinal Cord 60:1041–1049
157. Han S, Yin W, Li X, Wu S, Cao Y, Tan J et al (2019) Pre-clinical evaluation of CBD-NT3 modified collagen scaffolds in completely spinal cord transected non-human primates. J Neurotrauma 36:2316–2324
158. El-Husseiny HM, Mady EA, Hamabe L, Abugomaa A, Shimada K, Yoshida T et al (2022) Smart/stimuli-responsive hydrogels: cutting-edge platforms for tissue engineering and other biomedical applications. Mater Today Bio 13:100186
159. Arif ZU, Khalid MY, Zolfagharian A, Bodaghi M (2022) 4D bioprinting of smart polymers for biomedical applications: recent progress, challenges, and future perspectives. React Funct Polym 179:105374
160. Nazerian Y, Nazerian A, Mohamadi-Jahani F, Sodeifi P, Jafarian M, Javadi SAH (2023) Hydrogel-encapsulated extracellular vesicles for the regeneration of spinal cord injury. Front Neurosci 17:1309172
161. Najafi H, Farahavar G, Jafari M, Abolmaali SS, Azarpira N, Tamaddon AM (2024) Harnessing the potential of self-assembled peptide hydrogels for neural regeneration and tissue engineering. Macromol Biosci 24:e2300534

Figures

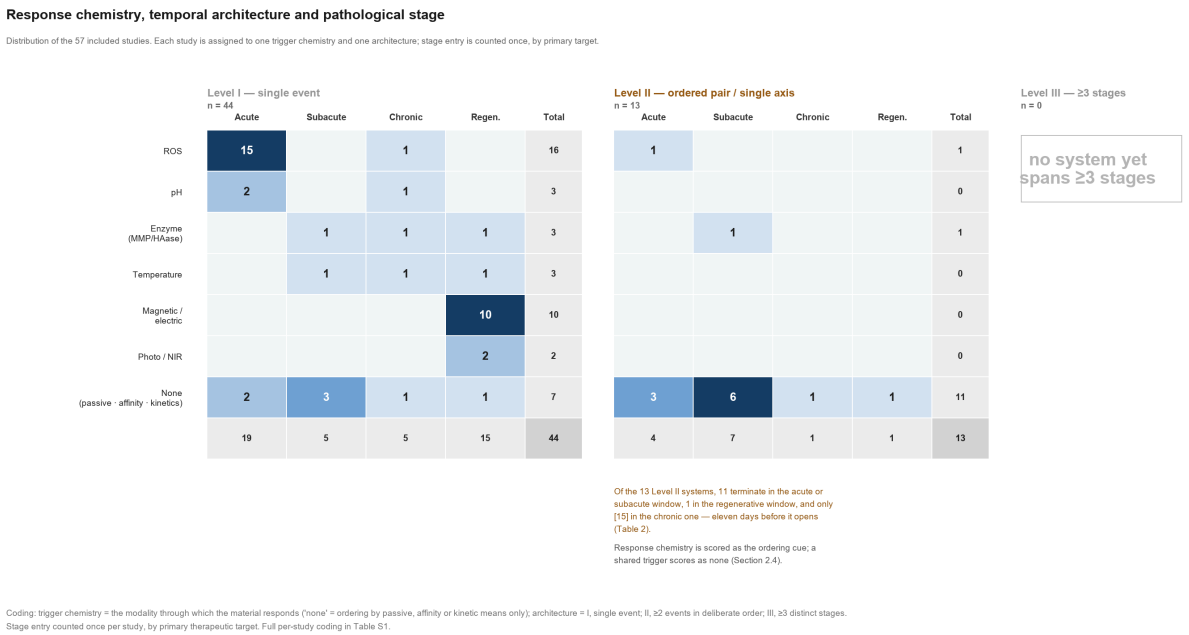


Figure 1

Distribution of the 57 included studies across response chemistry (rows), temporal architecture (panels: Level I, single event; Level II, two or more events in a deliberate order; Level III, three or more distinct pathological stages) and pathological stage (columns within each panel). Each study is assigned to one trigger chemistry and one architecture, and enters the stage count once, by primary therapeutic target. “None” denotes systems in which no distinct chemical cue orders the later event: the sequence is passive, affinity-based, or set by release kinetics. A system whose events share a single gate is

grouped here as well, because a shared cue creates no order, and [32] is the example: three releases from one ROS trigger. The chronic column is not empty—ten studies engage that stage—but only six take it as their primary target, and it is the stage designated as endpoint by just one two-event program: of the 13 Level II systems, 11 are designed to terminate in the acute or subacute window, one ([15]) in the chronic one—which it does not reach in time (Table 2)—and one in the regenerative window. Level III remains unoccupied. Full per-study coding is given in Supplementary Table S1.

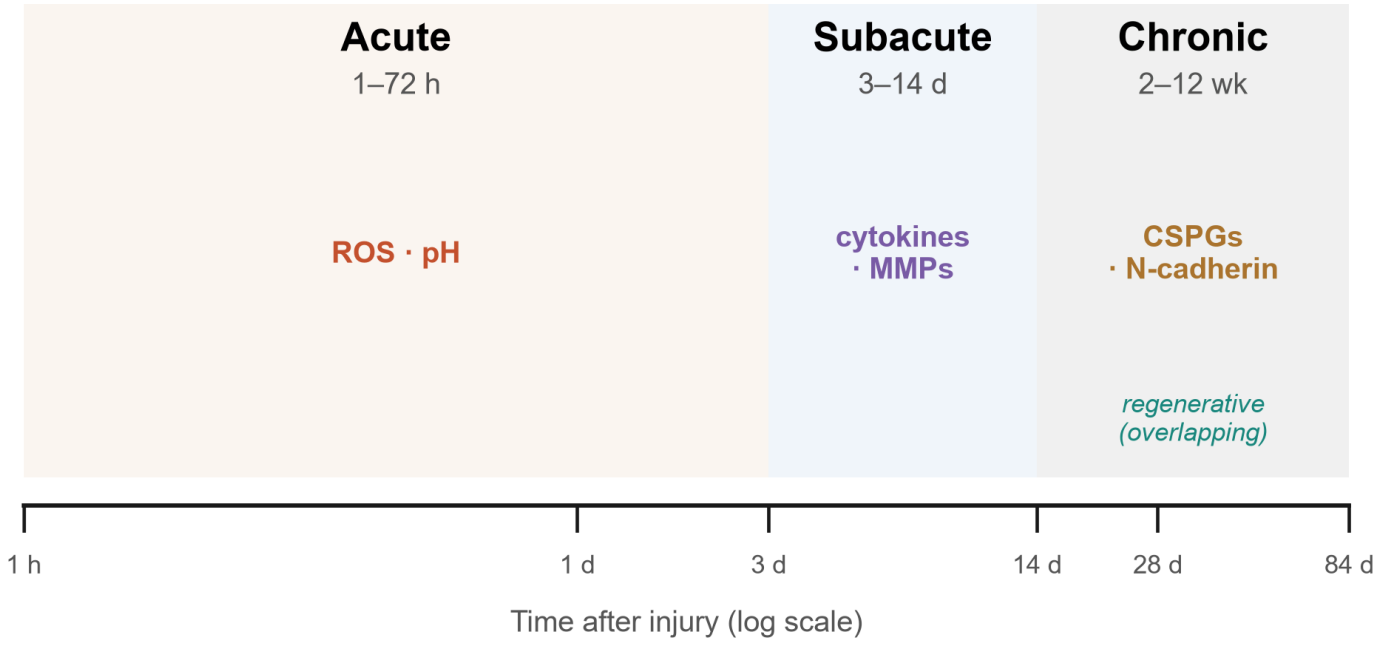


Figure 2

The spatiotemporal pathophysiology of SCI as a temporal coordinate system: four stages (acute, subacute, chronic, regenerative), each defined by stage-specific molecular signals (ROS, pH; cytokines, MMPs; CSPGs, N-cadherin; pro-differentiation signals) that serve as the endogenous “clock” a responsive hydrogel can sense. The stages overlap in time rather than following one another cleanly: the regenerative axis opens while the chronic barrier is still consolidating, and that overlap, rather than any single boundary, is what a staged material has to negotiate.

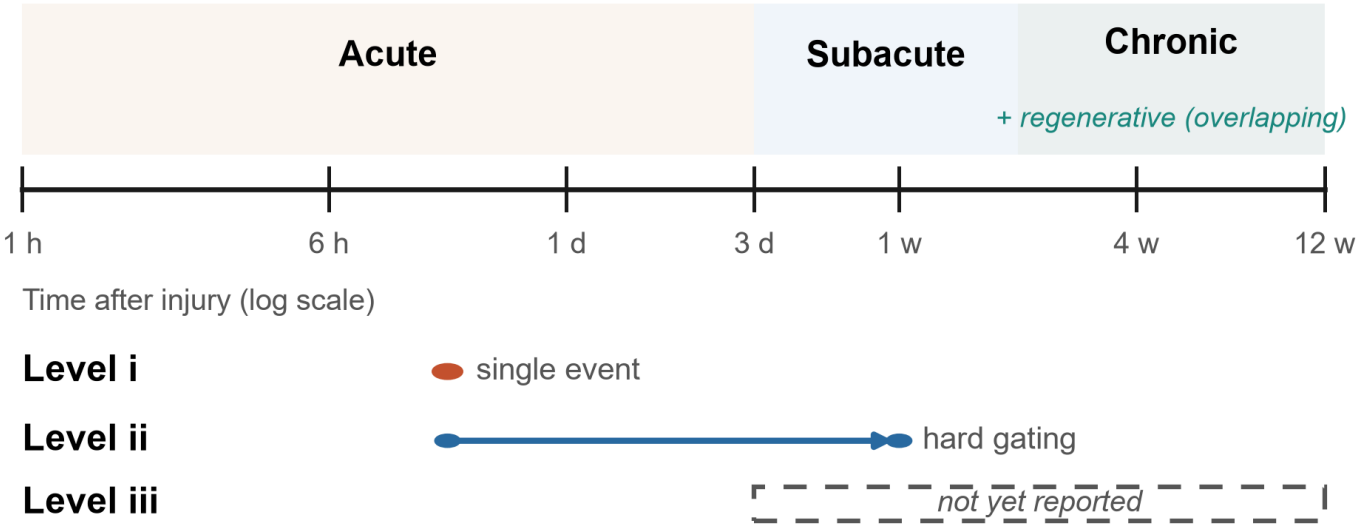


Figure 3

A three-level hierarchy of temporal programming, drawn on the same logarithmic time axis as Fig. 2. Level I systems sense one cue and act once, lighting a single point on the timeline. Level II systems encode two events in a deliberate order, either by hard gating (solid arrow; the second event is chemically triggered only once the first has occurred, e.g. ROS→MMP) or by engineered sequencing (dashed arrow; the second event is simply scheduled later, e.g. Ang-(1–7)→NT-3), and the latter is open-loop. Level III systems would span three or more distinct pathological stages; no such system has been reported, and the track is therefore drawn dashed.

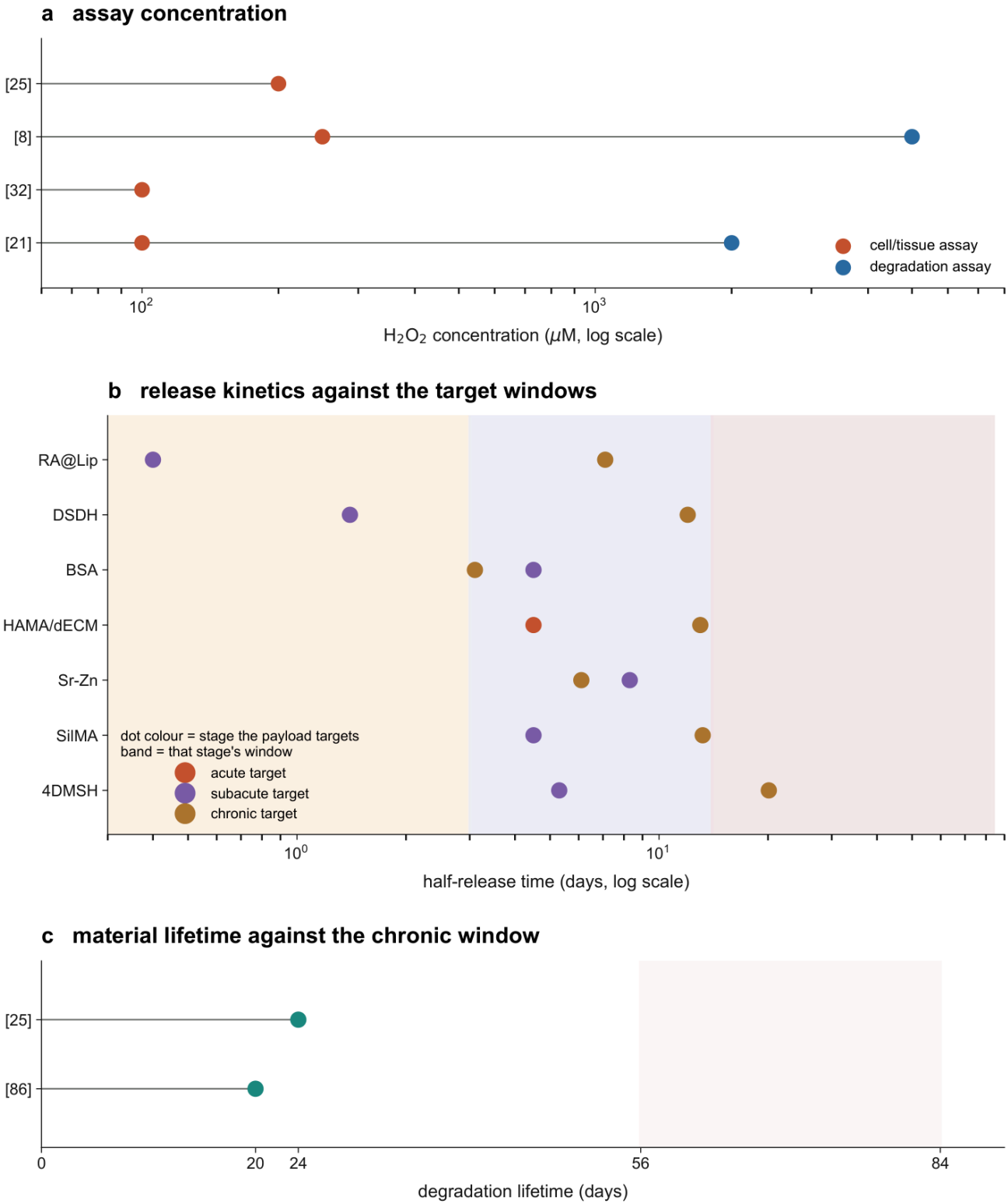


Figure 4

The three design parameters, anchored to values reported by the surveyed systems. Top: the H_2O_2 concentrations used in experimental cell and tissue assays cluster at 100-250 µM ([21] 100 µM; [32] 100 µM; [8] 250 µM; [25] 200 µM), whereas degradation and scavenging assays run at 2-5 mM ([21] 2 mM; [8] 5 mM). Middle: release kinetics measured across seven systems ([22][15][87][86][138][139][32]), with the windows of Section 3 above the axis; in every system the payload released first reaches half release between 0.4 and 6.1 days and the slower one between 4.5 and 20.1 days (Table 2). Bottom: measured degradation lifetimes under oxidative conditions ([86] 20 d; [25] 24 d) against the 8–12 weeks over which the scar matures, the late part of the chronic window fixed in Section 3.5. Because the assays are run one to two orders of magnitude above the concentrations a lesion sustains, a threshold tuned to the assay and one tuned to the lesion are not interchangeable.

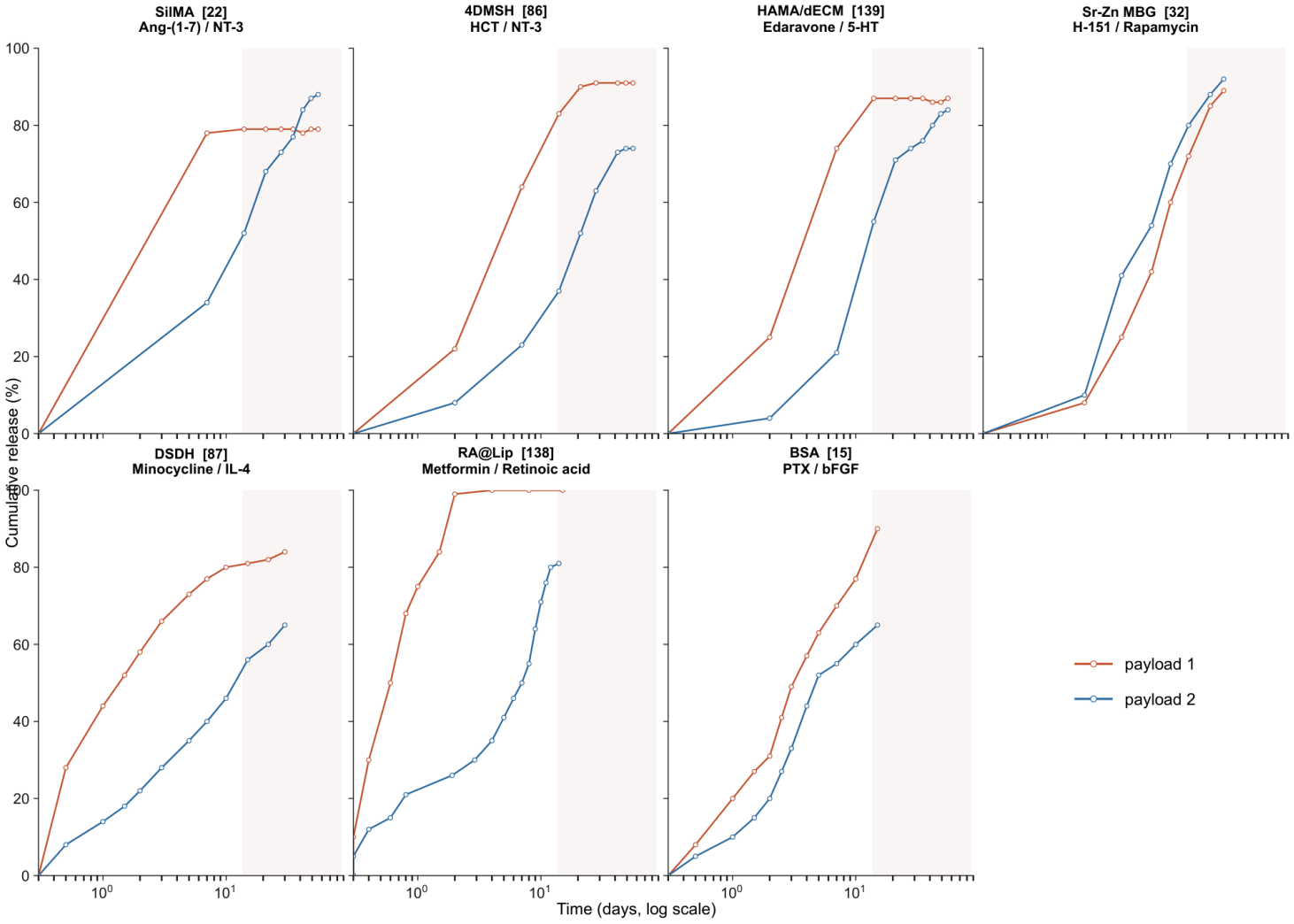


Figure 5

Cumulative release of the two payloads in seven staged systems, plotted on a common logarithmic time axis (1-56 days). Panels are labelled with the reference number of the source study; the shaded band marks the chronic window of Table 2 (days 14–84), shown as far as the plotted axis extends. Values were read from the published curves (SilMA, Fig. 2E of [22]; 4DMSH, Fig. 4B of [86]; HAMA/dECM, Fig. 3K of [139]; Sr-Zn MBG, Fig. 2b-c of [32]; DSDH, Fig. 4c of [87]; RA@Lip, Fig. 3K of [138]; BSA, Fig. 7B of [15]), and t½ was obtained by linear interpolation between the two sampling points that bracket 50% of cumulative release, with no curve fitting.

Temporal matching nomogram

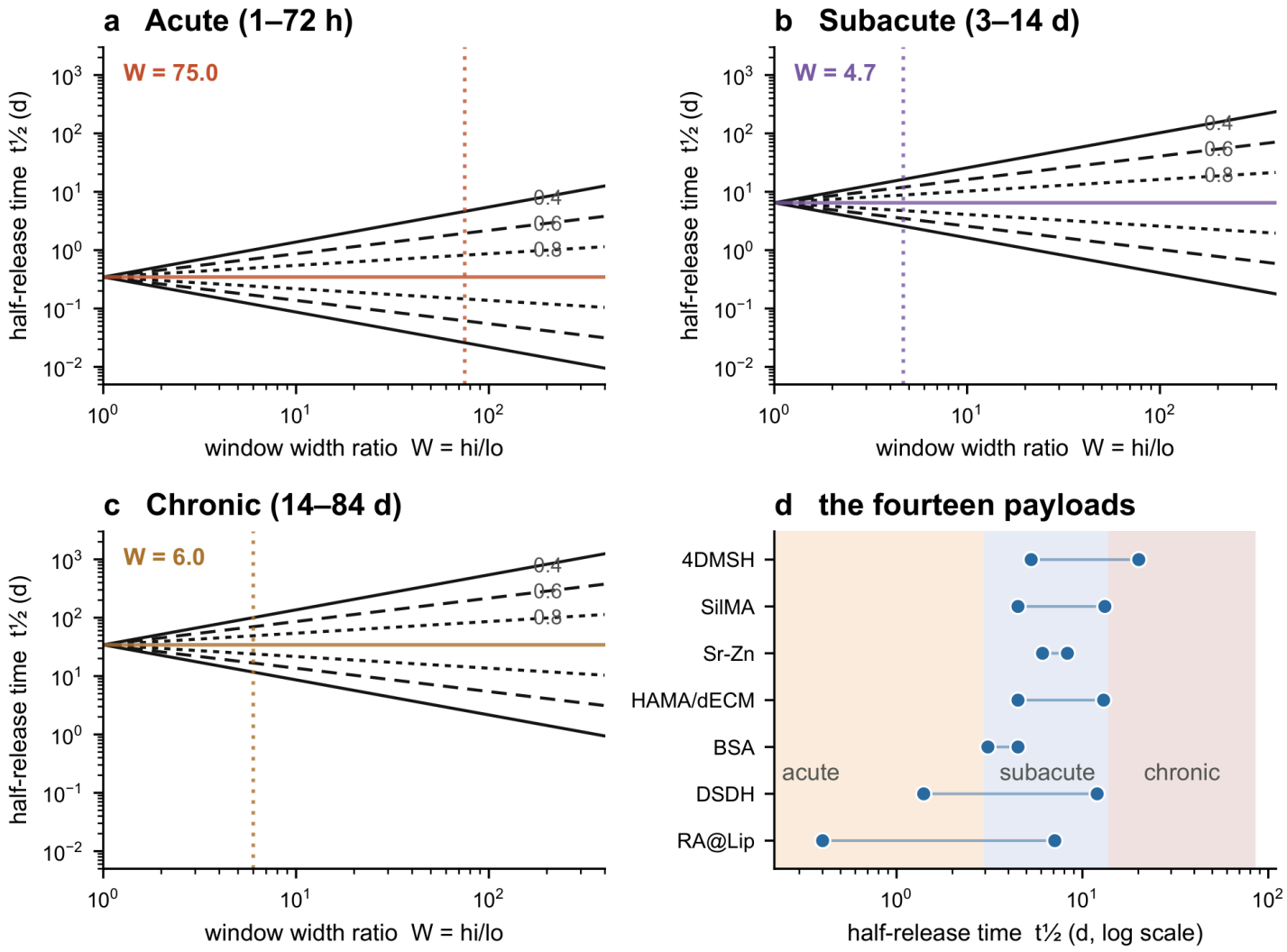


Figure 6

Temporal matching nomogram. Panels a–c give the relation between window width ratio W and half-release time for the acute, subacute and chronic windows; each pair of branches is one contour of the matching index (0.4 solid, 0.6 dashed, 0.8 dotted), and the horizontal line marks the midpoint of the window. Panel d places the fourteen payloads of Table 2 on the same logarithmic time axis as the three windows, one row per system, so that the distance between the two members of a pair is Δt½.

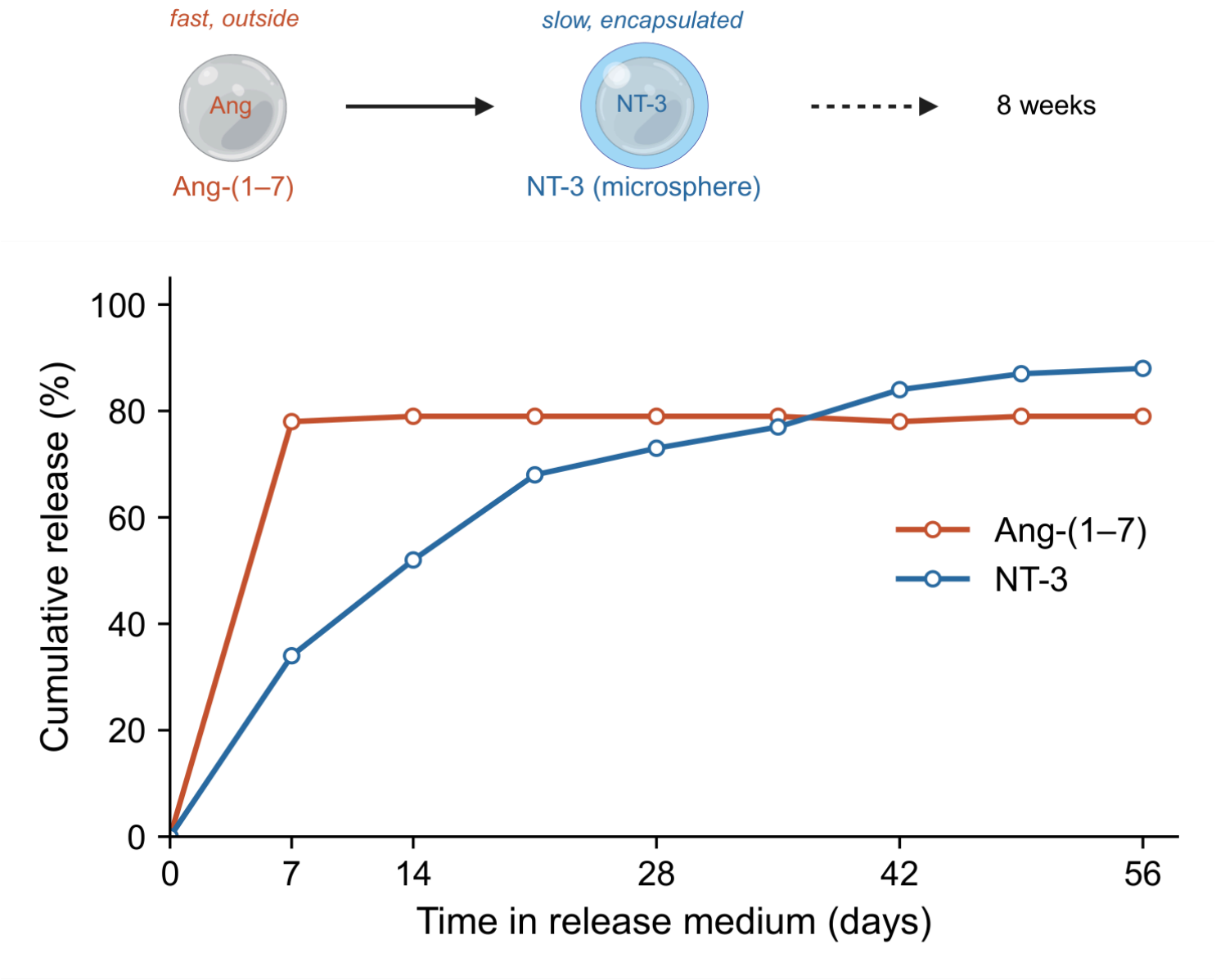


Figure 7

Dual-phase release from the SilMA system, digitised from Fig. 2E of [22]; the same SilMA release data are replotted on a logarithmic axis in Fig. 5. Angiotensin-(1-7) reaches about 78% of cumulative release within the first week, covering the inflammatory window in which M2 polarization is required; NT-3 remains below 40% at that point and is delivered over the following weeks, through the regenerative window. The hand-off is produced by differential release rates from a single scaffold and is therefore open-loop: neither step is triggered by a change in the lesion.

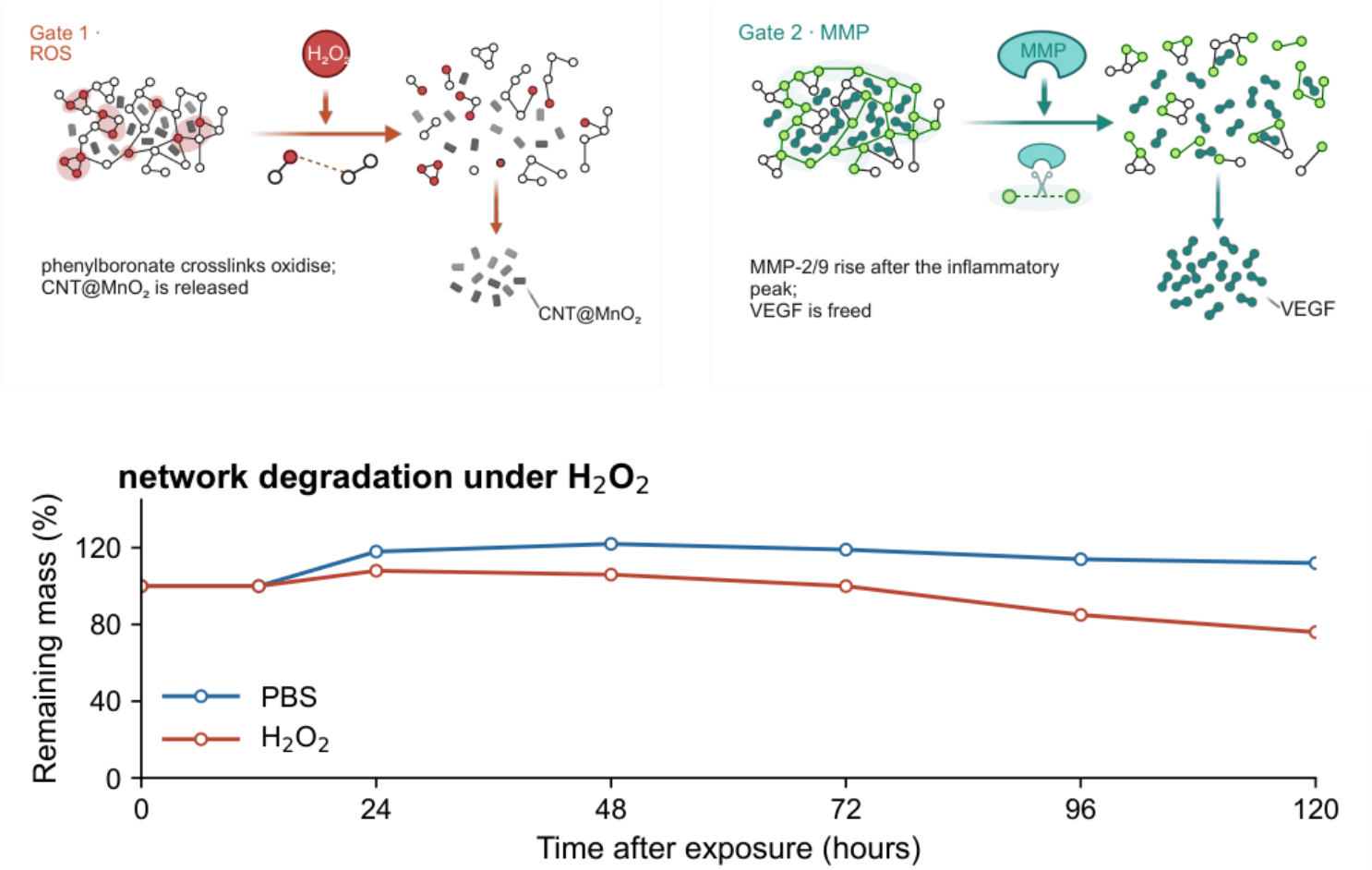


Figure 8

The cascade in two gates, and the evidence that the first gate opens. Top left: Gate 1. H_2O_2 oxidises the phenylboronate crosslinks, the network loses its integrity, and CNT@MnO_2 is released. Top right: Gate 2. MMP-2/9 accumulates after the inflammatory peak and cleaves the peptide linker, freeing VEGF; the second gate therefore opens only on a cue that Gate 1 has already made possible. Bottom: remaining mass of the PVA/TSPBA network under H_2O_2 (ROS present) versus PBS, digitised from Fig. 3g of [21]; oxidative cleavage of the phenylboronate crosslinks removes about 24% of the network by 120 h, whereas the PBS control swells rather than degrades. Only the first gate is quantified in the source figure; the cumulative VEGF release curve is not reported in the main text of [21].

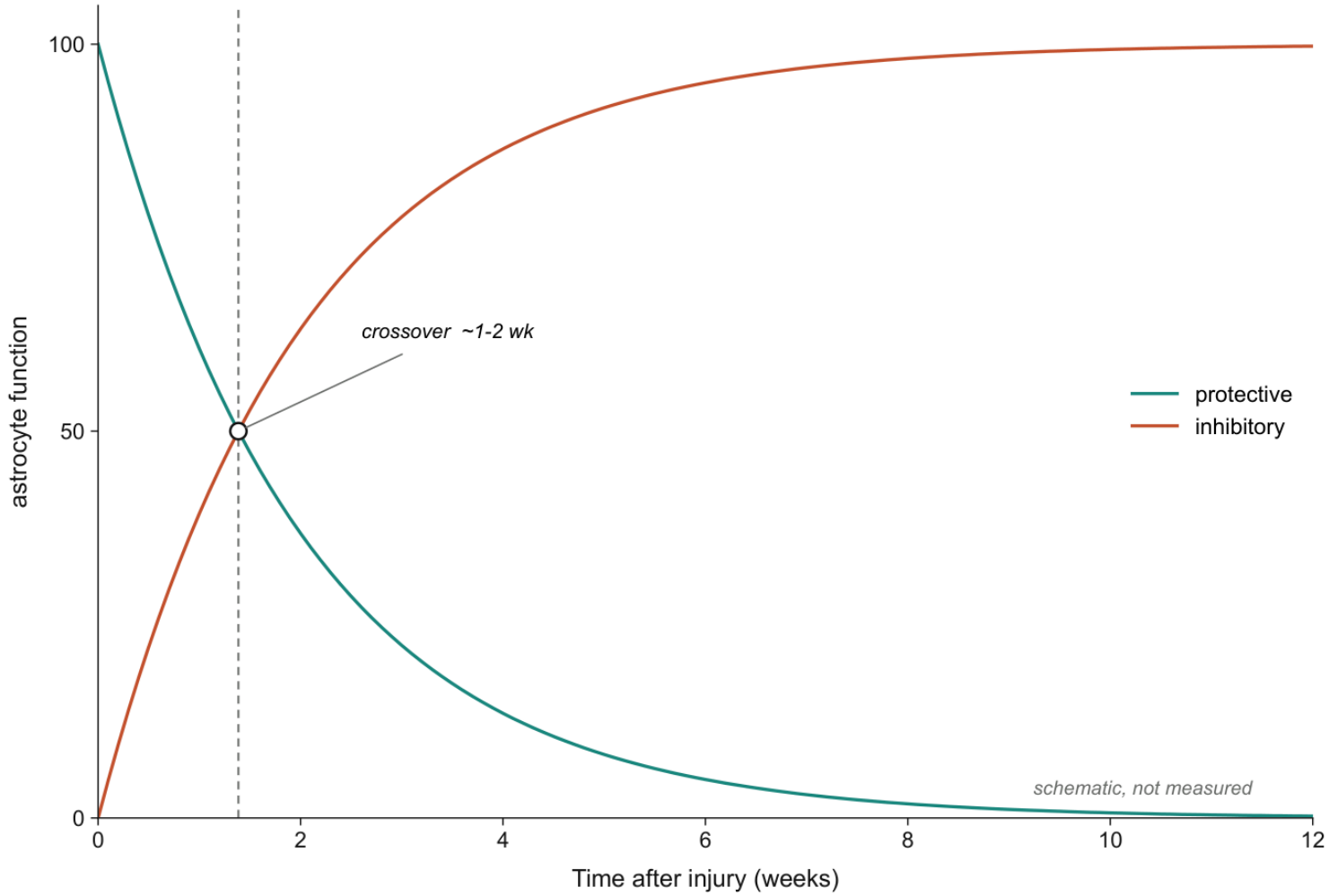


Figure 9

The chronic-stage dilemma: a problem of timing rather than of target. Reactive astrogliosis is protective early and inhibitory late, and the two functions cross at roughly 1–2 weeks (curves are schematic and are not plotted from measured values). Both molecular strategies described in Section 5.3—sustained inhibition of Pin1 and blockade of integrin–N-cadherin aggregation—are delivered continuously from implantation and therefore act across both regimes, including the early phase in which the barrier is still protecting spared tissue. The therapeutically relevant target is the later, growth-blocking consolidation; neither strategy can be switched on after the crossover, and neither supplies the second, ordered event that Level II would require.